NOAA Technical Memorandum ERL PMEL-20

METLIB - A PROGRAM LIBRARY FOR CALCULATING AND PLOTTING MARINE BOUNDARY LAYER WIND FIELDS

J. E. Overland
R. A. Brown
C. D. Mobley

Pacific Marine Environmental Laboratory
Seattle, Washington
June 1980

UNITED STATES
DEPARTMENT OF COMMERCE
Philip M. Klutznick, Secretary

NATIONAL OCEANIC AND
ATMOSPHERIC ADMINISTRATION
Richard A. Frank, Administrator

Environmental Research
Laboratories
Wilmot N. Hess, Director

NOTICE

The Environmental Research Laboratories do not approve, recommend, or endorse any proprietary product or proprietary material mentioned in this publication. No reference shall be made to the Environmental Research Laboratories or to this publication furnished by the Environmental Research Laboratories in any advertising or sales promotion which would indicate or imply that the Environmental Research Laboratories approve, recommend, or endorse any proprietary product or proprietary material mentioned herein, or which has as its purpose an intent to cause directly or indirectly the advertised product to be used or purchased because of this Environmental Research Laboratories publication.

CONTENTS

METLIB - A PROGRAM LIBRARY FOR CALCULATING AND PLOTTING MARINE BOUNDARY LAYER WIND FIELDS*

J. E. Overland
Pacific Marine Environmental Laboratory
Seattle, Washington

R. A. Brown
C. D. Mobley
University of Washington
Seattle, Washington

METLIB is a FORTRAN program library for deriving earth-located time series of geostrophic, gradient, or surface winds from sea level pressure (SLP) and ancillary fields gridded on a polar stereographic projection. Such fields are generated at the National Meteorological Center (NMC) and at Fleet Numerical Oceanographic Central (FNOC). They can also be generated by digitizing SLP charts analyzed manually. The library also contains programs for contouring scalars, such as SLP or wind speed, and for plotting vector arrows with a map background. Plotting is based upon the NCAR graphics routines. A major advantage to the library is that spherical geometric calculations involving polar stereographic grids are internal to the programs. The relationship between gradient wind and surface wind can be assigned from speed reduction and turning angle constants or by a baroclinic, stability-dependent, single point boundary layer model.

1. INTRODUCTION

This document provides an introduction to the program library, discusses the data structure used by the library, and provides documentation of the geophysical algorithms used to derive various parameters and perform geometric calculations. It provides a description of the SUBMIT files for accessing the library as of date of publication. The library is divided into four program divisions, UNPACK or DECKS, WINDS, PTWIND, and PLOTGRD and two subroutine libraries, WSUBLIB and those called by PLTPROC.

*Contribution No. 451 from NOAA/ERL Pacific Marine Environmental Laboratory.

UNPACK extracts data from a larger data set, normally tapes such as those supplied by NCAR or NMC, and creates a master file in a standard format for all subsequent programs. DECKS performs the same function as UNPACK for card or terminal input of fields that have been digitized from manual analyses. Program WINDS inputs a series of sea-level pressure (SLP) fields in standard format and, depending upon the option, can also input air temperature, air-sea temperature difference and dew point depression fields. It outputs u and v components at each grid point. Output winds can be geostrophic, gradient, empirical reduction and turning of the gradient wind, or calculated from a planetary boundary layer (PBL) model. Two of the three PBL models have the option of outputing stress or heat flux in place of surface wind. PTWIND can take u and v fields generated by WINDS, interpolate them to any specified latitude and longitude, and convert the grid components to speed and direction relative to north. PLOTGRD can input and contour up to two scalar fields and can plot their difference. It can draw arrow plots of a vector field or the difference of two vector fields, and can plot a vector field with contours of a scalar, including contours of the magnitude (isotachs) of the vector field itself or the difference in magnitude of two vector fields. All routines are intended to be machine-independent FORTRAN programs.

For use at PMEL or other locations with access to the Environmental Research Laboratories' CDC 6600 computer in Boulder, Colorado, SUBMIT files are shown for WINDS, PLOTGRD and their combination. These SUBMIT files are specific to the NOS 1.3 operating system in use at the time of publication. RWINDS submits WINDS and RPLOT submits PLOTGRD. PLOTW inputs scalar fields, calculates wind fields and plots the results (i.e., runs WINDS and PLOTGRD together). PLOT2W inputs scalars, runs WINDS twice, and plots vector differences. PLOT2W2 inputs two separate sets of SLP scalars, calculates winds for each and plots their difference.

2. DATA SOURCES

NMC currently produces SLP and surface air temperature (SAT) analyses at 0000 and 1200 GMT on one of two polar stereographic meshes: the PE 65 x 65 point grid, with a spacing of 381 km at 60°N covering the northern

hemisphere; and the LFM 53 x 57 point grid, a fine-mesh grid with a spacing of 190.5 km at 60°N, covering North America and the adjacent waters (Fig. 1 and 2). PE and LFM are historical names standing for "Primitive Equation" and "Limited Area Fine-Mesh Model". The PE data are archived at the National Center for Atmospheric Research (NCAR) (Jenne, 1975) and the National Climate Center (NCC). At present the LFM data are not routinely archived for general distribution. Pressure fields are also produced by Fleet Numerical Oceanographic Central (FNOC) on a 63 x 63 point grid with the same scale and orientation as the PE grid. All grids are uniformly spaced upon a polar stereographic map projection, which preserves angles.

Over the ocean, SLP and SAT values for operational forecast models are obtained from ocean-station vessel, buoy and ship observations analysed by a variety of objective analysis techniques (Cressman, 1959; Flattery, 1970; Holl and Mendenhall, 1971). For many research purposes it is necessary to reanalyze the SLP charts making use of reports that were not included in the NMC analysis. To this end, the reanalysis is done on a standard polar stereographic projection (either the PE or LFM) and digitized at a uniform spacing compatible with the program library.

Internal north-pole coordinates are (33,33) for the present PE grid and (27,49) for the LFM. The FNOC pressure fields use pole coordinates of (32,32). For PE data prior to 1976 the NMC "octagon" was used. The number of grid points was 47 x 51, the pole location was (24,26), and the data were stored in a one-dimensional array. This is the format used by NCAR to store much of their NMC PE data.

3. DATA MANAGEMENT

All master data files created by UNPACK or DECKS are in a standard format for subsequent analysis routines. Master data sets are arranged chronologically and separated by type (e.g., SLP or wind speed) and geographical region (e.g., the Gulf of Alaska). Thus, one file might have a 1-yr time series of observed SLP's in a 10 x 10 grid for the Gulf of Mexico; another file might consist of model-generated, u-component winds for the same period, etc.

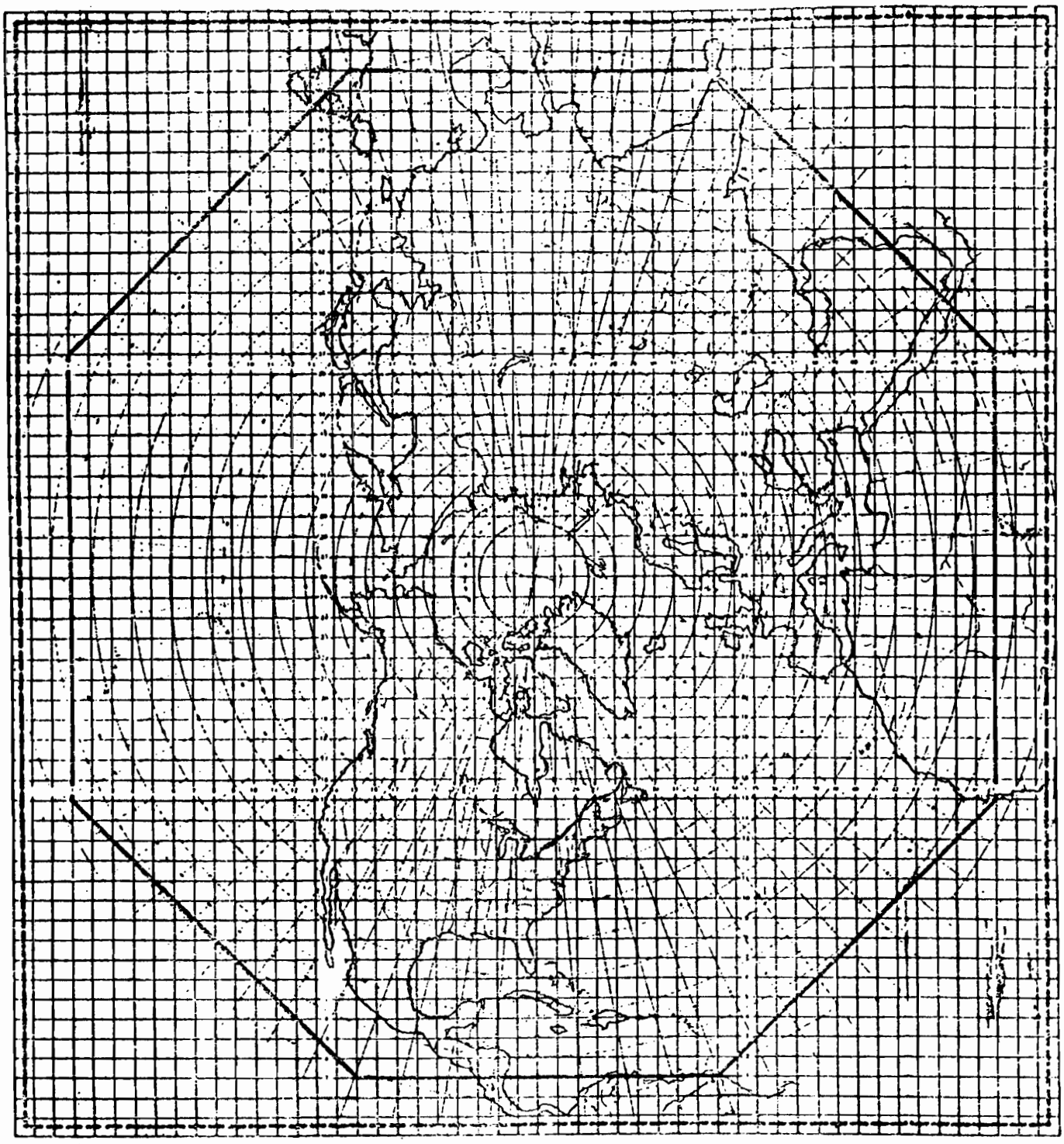

Figure 1. The NMC octagon 47 x 51 point grid. The 65 x 65 grid in present use has the same mesh point locations but covers a larger area.

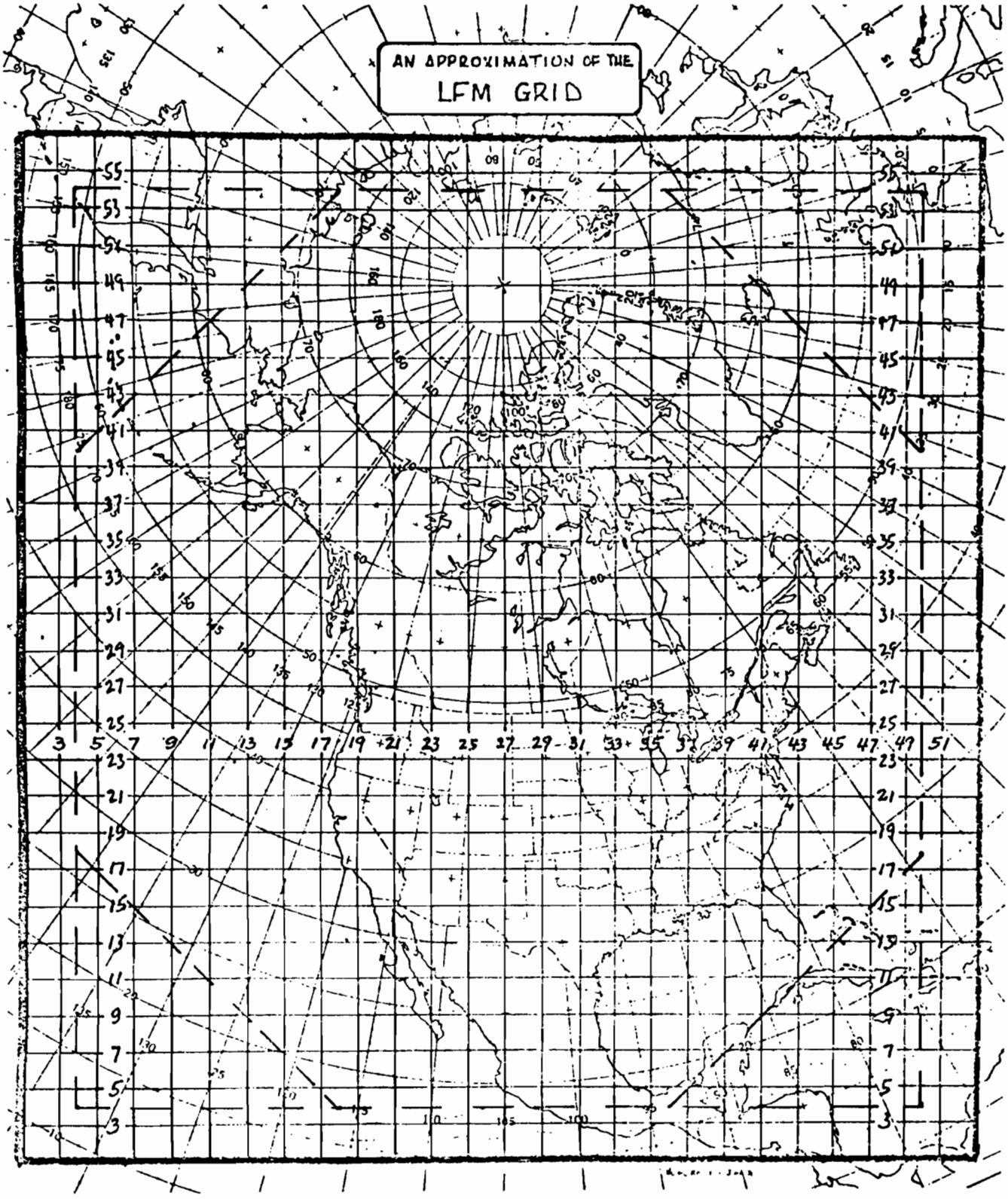

Figure 2. LFM 53 x 57 point grid (NMC).

All records are generated by FORTRAN unformatted write statements and are stored in an unpacked form. Every file is identified by a file header. This header consists of six words and identifies the particular grid on which the data are stored:

Word	Quantity
1	IGRID. Identifies the grid used: 1 means PE IGRID = 2 means LFM 3 means NMC octagonal (PE) 4 means FNOC
2,3	XIS,XJS. The (I,J) coordinates (relative to the above grid) of the lower left corner of the data subregion.
4,5	IMC,JMC. The (I,J) dimensions of the coarse (uninterpolated) grid subregion covered by the data.
6	IFACT Specifies the degree to which the data have been interpolated relative to the standard mesh. 1 means no interpolation, i.e., same as PE or LFM IFACT = 2 means interpolation to 1/2 mesh 4 means interpolation to 1/4 mesh.

For example, if SLP were hand digitized on a grid twice as fine as the PE, IMC and JMC would equal the size of the equivalent coarse PE array, but IFACT would equal 2.

The header is followed by as many data groups as necessary. Each group consists of seven identification words followed by the data. The identification words specify the date and data characteristics as follows:

Word		Quantity
1	IYEAR.	"68" means 1968
2	MONTH.	"11" means November
3	IDAY.	
4	IHOUR.	"12" means 12 GMT
5	ITYPE.	Data type coded as in NMC office note 84 (1973): 8 pressure in mb 16 air temperature in °K 18 dew point depression in °K

		30 air-sea temperature difference in °K
		48 u wind component w/r to grid in cm s^{-1}*
		49 v wind component w/r to grid in cm s^{-1}*
		50 wind speed in cm s^{-1}*
		55 direction from which wind is blowing with respect to north in degrees
		148 u wind stress component relative to grid in dynes cm^{-2}
		149, 150, 155 same as 49, 50, 55 for stress
		180 Total heat flux in watts m^{-2}
		182 Latent heat flux in watts m^{-2}
		183 Sensible heat flux in watts m^{-2}
		384 Sea surface temperature in °K
6	IOBS.	Gives the type of forecast
	IOBS =	0 means observed data 12 means 12-hr forecast data 24 means 24-hr forecast data, etc. 910 means climate type 1.0 920 means climate type 2.0, etc.
7	IFLAG.	Flags missing data
	IFLAG =	0 means data are complete 1 means data are missing

Following these identification words, the data array is written in words 8, 9, 10, etc. Missing data are given the value 9999. Two-dimensional arrays, A(I,J), are structured so that I and J increase in the same direction as I and J of the weather forecasting grids, with A(1,1) at the lower left corner of the subregion and the arrays reading ((A(I,J), I=1, IMC), J=1, JMC).

*Note that standard NMC and SI. format is m s^{-1}.

4. MAIN PROGRAMS

4.1 Use of METLIB

METLIB consists of a collection of programs and subroutines along with a set of SUBMIT files to run them. These libraries and example files are stored under USER, METLIB on the ERL 6600 computer. This USER is meant for read-only storage of programs. All data files and personal copies of SUBMIT and main program files should be stored in separate USER areas. Normal procedure is to copy the desired files from METLIB into a new area and then modify the files as necessary for a particular application. This entails changing the SUBMIT files and the dimension statements of the main programs to match the data array size.

4.2 UNPACK (Used to Extract Subsets from Large Temporal or Geographic Data Sets such as NCAR)

UNPACK performs three tasks. It unpacks the data, if necessary; extracts the appropriate time series, subregion, data type, and forecast type as specified; and organizes the data set into the standard format for use by the subsequent analysis routines. Since the raw data tapes come in different formats, a separate UNPACK must be written for each grid used (NMC octagonal, FNOC, etc.). For the version of UNPACK that is compatible with the NMC octagonal grid obtained from NCAR, the user specifies the starting and stopping time of the file to be generated, the lower left-corner coordinates and dimensions of the region to be analyzed, the data type and the forecast types on an input data card (13I2) as follows:

IYSTRT. . . . The year of the first desired datum (e.g. 71 for 1971)
IMSTRT. . . . The month (e.g. 3 for March)
IDSTRT. . . . The day
IYSTOP. . . . The year of the last desired datum
IMSTOP. . . . The month
IDSTOP. . . . The day
ILL . . . . The lower left (I,J) coordinates measured on the NMC
JLL . . . . octagonal grid of the desired geographical region.
IMC . . . . The number of (NMC octagonal) grid points to be taken in

JMC — the I and J directions to cover the desired geographical region. The point (ILL,JLL) is counted as the first point. The dimension of array is IMC by JMC.

IFUNC . . . . The NCAR function code specifying the data type:
=10 for air temperatures
=28 for sea-level pressures
=47 for sea-surface temperatures.

IFCST . . . . The forecast type
=0 for observed data
=12 for 12-hr forecast data, etc.

ISMO . . . . =1,2,4 to interpolate the original data to a finer mesh.

The file generated by UNPACK is in standard format with a file header and a time series of data records.

4.3 DECKS (Creates a Standard Format File from Digitized Fields)

DECKS performs for manually digitized fields the same function that UNPACK performs for the NCAR data sets. A uniform mesh compatible with the locations of the grid points of either the LFM or PE is laid over a hand-analysed polar stereographic National Weather Service sea level pressure chart or hand analyses performed on charts produced by program MAP (section 4.6), and values are extracted. The grid can be either at the standard, half or quarter mesh spacing.

The first card read by DECKS gives IGRID, XIS, XJS, IMC, JMC, IFACT, ITYPE, N, OFACT on a (I3,2F3.0,6I3) format. The first six words are the standard header from section 3.0. The number of fields to be read is N. OFACT is the resolution of the digitized input fields relative to the standard PE or LFM resolution; OFACT can be 1, 2, or 4 with the same meaning as IFACT. If IFACT is greater than OFACT, the digitized fields will be interpolated to a finer mesh by biquadratic interpolation. This card is followed by the data sets, each beginning with a header card (6I2) specifying IYEAR, IMONTH, IDAY, IHOUR, IOBS, IFLAG, and the data read in (user specifies format):

```
      DO 10  J=1,JM
10    (ARRAY(I,J),I=1,IM)
```

In DECKS the dimension of ARRAY(IM,JM) is set at the size of the input array and the dimension of OUTPUT (IMM,JMM) and W(IMM,JMM) are set at the size of the array written on file in standard format. Values on the DATA statement following the DIMENSION statement must also be set.

4.4 WINDS (Calculations of Winds)

Program WINDS uses any of several models to compute surface wind fields. Input always consists of a time series of sea-level pressures defined at each point of a spatial grid. Models 6-9 require the time sequence of surface air temperatures and air minus sea-temperature differences. The Brown model has the option of dew-point depression fields as well. The information in the file header record on each data set (i.e., IGRID, XIS, XJS) completely defines the parameters necessary for geometric manipulations on the polar stereographic grid. Output consists of time series for u and v components of winds.

Figure 3 shows a sample SUBMIT file for running WINDS on the CDC 6600. TAPE10 has the grid-point pressure fields in standard format, while TAPE11, TAPE12 and TAPE13 have the surface air temperature, air-sea temperature difference, and dew point depression grid fields. TAPE14 and TAPE15 are the output u and v fields. WSUBLIB contains the library of all subsequently called subroutines. The input data card is in (4I2,I4,I2,2F5.1,I2) format. The parameters are:

IYSTRT. . . The year (e.g., 68) of the starting time
IMSTRT. . . The month (e.g., 11)
IDSTRT. . . The date
IHSTRT. . . The hour
KSETS . . . The number sets to be analyzed
MODEL . . . The model to be used to compute the surface winds. Values 1-5 are reserved for temperature-independent models. At present MODEL =
- 1 for geostrophic winds
- 2 for surface winds by the balance equation (Mahrt, 1975)

3 for gradient winds

4 empirical constants

6 use of Brown's model

8 use of Cardone's model.

CNST1 If MODEL = 4 is specified, CNST1 is the fraction of the gradient wind speed used as the surface wind speed and

CNST2 CNST2 specifies the inflow turning angle in degrees to the left of the geostrophic wind direction:

For MODEL = 6 or greater, CNST1 specifies the anemometer height (cm) assumed for the calculations. CNST2 specifies the default relative humidity (decimal fraction).

If MODEL = 6 and CNST2<0, dew-point depression will read from TAPE13.

ICNST = 0 wind components as output on TAPE14 and 15

= 1 wind stress components as output

= 2 total heat flux and latent heat flux

= 3 total heat flux and sensible Heat flux.

The value for ITYPE written on the output files is

ITYPE = 480 + MODEL for the u velocity component

490 + MODEL for the v velocity component

500 + MODEL for the u stress component

510 + MODEL for the v stress component

520 + MODEL for total heat flux

530 + MODEL for latent heat flux

540 + MODEL for sensible heat flux

so that ITYPE = 482 designates a surface u field generated by MODEL = 2. The only program changes that need to be considered are array dimensions in WINDS.

```
00100 /JOB
00110 EXAMPLE,T270,
00120 ACCOUNT(METLIB)
00130 CHARGE(RP)
00140 GET,WINDS/UN=METLIB.
00150 GET(TAPE10=SLP)
00160 GET(TAPE11=SAT)
00170 GET(TAPE12=ASTD)
00180 GET,TAPE13=DPTD.
00190 GET(WSUBLIB/UN=METLIB)
00200 FTN,I=WINDS,R=3.
00210 LDSET(LIB=WSUBLIB)
00220 LGO.
00230 REPLACE(TAPE14=UFIELD)
00240 REPLACE(TAPE15=VFIELD)
00250 /EOR
00260 68110118   104  0.8 30. 00
 END OF INFORMATION ENCOUNTERED.
/
```

Figure 3. SUBMIT file RWINDS for running WINDS.

4.5 PTWND (Time Series of Winds)

PTWND inputs the u (TAPE14) and v (TAPE15) components of winds and creates time series of winds at up to five specific geographic locations by interpolation. The first data card is formatted (4I2,I4,2I2) and specifies the starting time, number of data sets in the time series, and the parameters NPT and IOUT:

NPT . . . Number of points at which the time series is to be created.

IOUT. . . Specifies whether u and v components of winds or speed and direction of winds are to be used.

IOUT = 0 for u and v components
1 for speed and direction.

Cards 2 through NPT+1 specify the latitude and west longitude (degrees) of each point in (2F5.1) format. Modifications to PTWND can be used to access the u and v fields for almost any purposes.

4.6 PLOTGRD (Plotting)

PLOTGRD is the main program for performing graphical analysis on the data sets generated by the METLIB wind analysis routines. Both scalar and vector fields can be processed in a number of ways, and contour plots and vector fields can be drawn on a continental outline background.

The primary purpose of PLOTGRD is for the user to set up arrays with the proper dimensions. All subroutines use variable-dimensioned arrays and need not be changed when data sets are changed.

The secondary purpose of PLOTGRD is to set default values for a number of parameters which control the plotting. These values can be changed as desired by the user.

Figure 4 shows a listing of RPLOT, the SUBMIT file for running PLOTGRD. The program uses up to six arrays corresponding to a first and second scalar field and u and v components for two vector fields. The

```
00100 /JOB
00110 EXAMPLE,T270.
00120 USER,METLIB.
00130 CHARGE,RP.
00140 GET,MAIN=PLOTGRD.
00190 GET,TAPE11=BSLP.
00191 GET,TAPE12=BSAT.
00192 GET,TAPE13=U6.
00193 GET,TAPE14=V6.
00194 GET,TAPE15=U1.
00195 GET,TAPE16=V1.
00230 GET,PLTPROC/UN=METLIB.
00231 CALL,PLTPROC(PLOTTER=1TK4010)
00232 REPLACE,TAPE2=EXAMPLT.
00290 /EOR
00300 0,0,0,3,2,3
00310 0,0,0,0,1,0
00320 10FINAL TEST
```

Figure 4. SUBMIT file RPLOT for running PLOTGRD.

logical unit numbers are assigned as TAPE11 through TAPE16. These files only need be attached if they are to be used. For example for plotting vectors only, TAPE11 and TAPE12 may be omitted.

The "PLOTTER=" parameter specifies the device which will perform the plotting:

PLOTTER = 1TK4Ø1Ø specifies a Textronics 4Ø1Ø terminal
PLOTTER = 1CCWIDE specifies a CALCOMP plotter with wide paper
PLOTTER = 1CCNARO specifies a CALCOMP plotter with narrow paper.

The first data card specifies what plots are to be made. The second card specifies the starting time and the number of plots to be made. Cards 1 and 2 are read as list-directed (free format) input, so data values need only be separated by commas or blanks. Card 3 is optional and is used to specify an additional title for the bottom of the plot.

Data Card 1:

Variable	Value	Comment
IS1	0	no scalar fields are to be processed. If IS1=0, set IS2=IS12=0 also.
	1	scalar field 1 (array S1) is to be contoured.
	2	scalar field 1 is to be read in but is not to be contoured (i.e., is to be used only for differencing, see IS12).
IS2	0	no second scalar field is to be processed.
	1	scalar field 2 is to be contoured.
	2	scalar field 2 is to be read in but not contoured.
IS12	0	the difference of the scalar fields S1-S2 is not to be contoured.
	1	the difference S1-S2 is to be contoured.
IV1	0	no vector fields are to be processed, if IV1=0, set IV2=IV12=0 also.
	1	wind vectors (arrows) only are to be drawn for vector field 1 (arrays U1 and V1).

	2	vector field 1 is to be read in but not processed (i.e., is to be used only for differencing, see IV12).
	3	isotachs only of vector field 1 are to be drawn.
	4	both 1 and 3, i. e., both arrows and isotachs of vector field 1 are to be drawn.
IV2	0	controls processing of vector field 2 the
	1	same as IV1 controls processing of vector
	3	field 1.
	4	
IV12	0	no differencing of vector fields is to be done.
	1	arrows only of vector field 1 minus vector field 2 are to be drawn.
	2	isotachs only of magnitude of vector field 1 minus magnitude of vector field 2 are to be contoured.
	3	both 1 and 2, i.e., arrows and isotachs of the differences.

Data Card 2:

Variable	Value	Comment
IYSTRT	0	If plotting is to begin with the first data set found on the input data files. Otherwise IYSTRT gives the year of the beginning time for data processing, e.g. 71 for 1971.
IMSTRT	0	As for IYSTRT, if plotting is to begin with the first data set. Otherwise, IMSTRT gives the month of the beginning time, e.g. 6 for June.
IDSTRT	0	As for IYSTRT. Otherwise, IDSTRT gives the starting day of the month, e.g. 15.
IHSTRT	0	As for IYSTRT. Otherwise IHSTRT gives the hour of the beginning time, e.g. 12 for 1200Z.

KSETS	0	If all data from the starting time until the end of the input data files are to be processed. If KSETS is greater than zero, then KSETS of data will be processed, beginning with the data set at time IYSTRT, IMSTRT, IDSTRT, IHSTRT. Note that setting IYSTRT=IMSTRT=IDSTRT= IHSTRT=KSETS=0 means that all data found on the input files will be processed.
IBACK	0	no background of continental outlines is to be drawn.
	N	Where N = 1,2, etc. a continental outline is to be drawn every Nth map.

Data Card 3: This card provides any desired title at the bottom of the plot, given the specification of 2 variables:

Variable	Format	Comment
NAUXTL	I2	The number of characters in the auxiliary title.
AUXTIT	7A10,A8	The character string which comprises the title. Up to 78 characters are allowed.

If no auxiliary title is desired, either omit this data card entirely or give NAUXTL the value 0. An example of data card 3 is: 13EXAMPLE TITLE.

After running the example RPLOT of Figure 4 (via SUBMIT, RPLOT, E=PMEL), one can view the generated plots on a Textronix terminal by typing

```
GET,EXAMPLT.
LNH, F=EXAMPLT.
```

If PLOTTER=1CCNARO is specified in RPLOT, then type

```
GET,EXAMPLT
```

ROUTE, EXAMPLT, DC=PR, UN=PMELTRM to send the plot to the CALCOMP plotter PMEL.

Figures 5 and 6 are sample plots.

The next set of variables is assigned within PLOTGRD (Fig. 7) and can be changed by editing a copied version of the program.

JGRID . . . . The interval for drawing latitude and longitude lines. Default is 10°.

IUSOUT. . . . Determines whether or not US state outlines are to be drawn if continental outlines are drawn. Default of 1 gives state outlines. Set to 0 for no outlines.

IDOT. . . . . 0 for continental outlines drawn by solid lines (default) 1 for continental outlines drawn by dotted lines

NHI . . . . . 0 if highs and lows are labelled by H and L respectively on all contour maps (pressure maps are always labelled H and L). -1 if highs and lows are not to be labelled (default).

Contour intervals for various types of data are as follows:

PRESIN. . . . The contour interval for pressure fields. Default is 4.0 mb.

TEMPIN. . . . The contour interval for temperature fields. The default is 1.0°C.

WINDIN. . . . The contour interval for isotachs of the wind fields. Default is 400.0 cm sec^{-1}.

OTHRIN . . . The contour interval for any other data type. The default of 0.0 allows the NCAR routine to examine the data and choose an appropriate interval.

Contour intervals for differences of data fields are as follows:

PDIFIN. . . . The contour interval for contouring the differences of two pressure fields. Default is 2.0 mb.

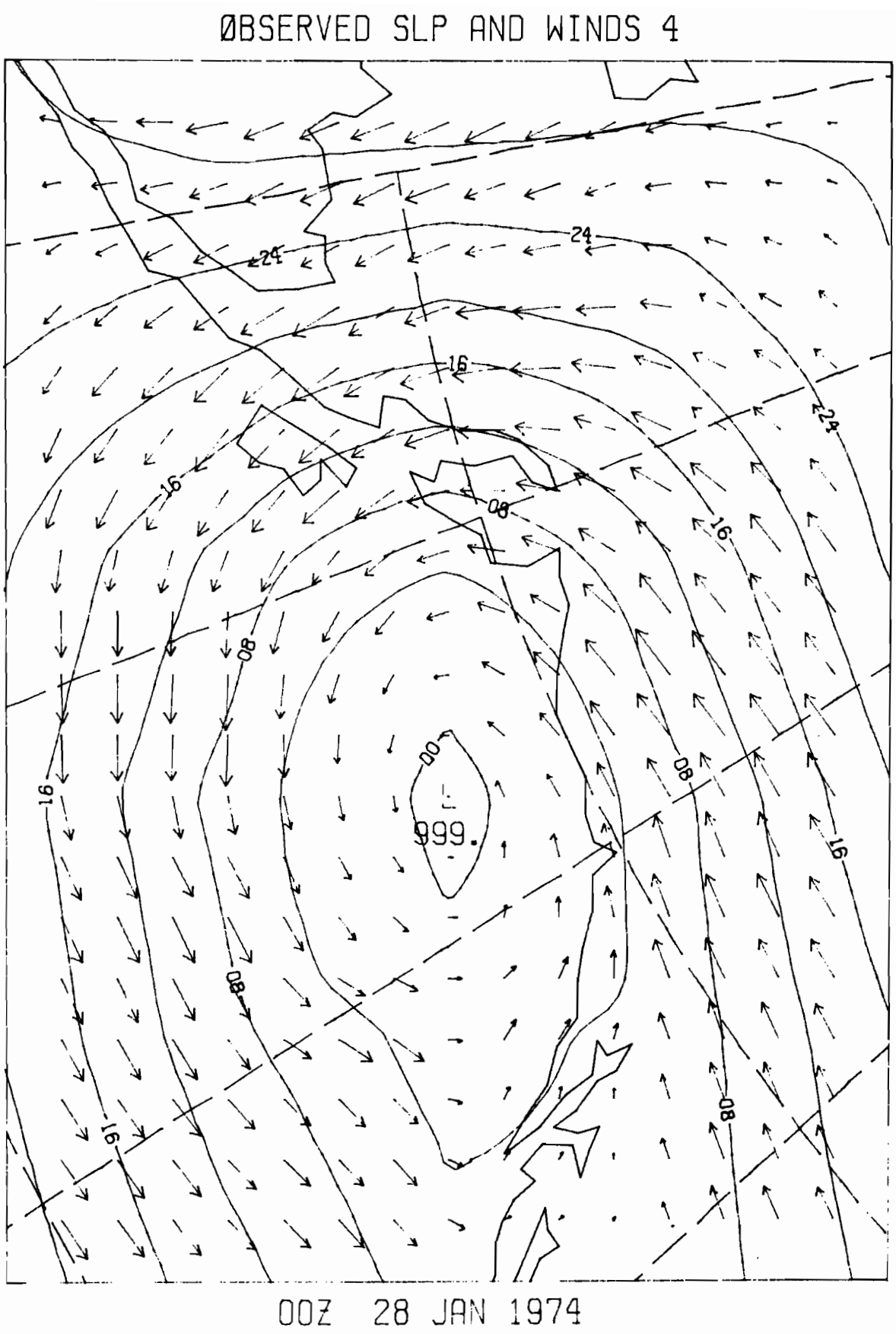

Figure 5. Winds generated by model 4 and pressures plotted for in the Gulf of Alaska.

Figure 6. Winds generated by model 2 and pressures plotted for in the Gulf of Mexico.

```
C      **********  BEGINNING OF USER DEFINED SECTION  **********
C
C     SET ARRAY DIMENSIONS
C
      DIMENSION S1(21,25),S2(21,25)
      DIMENSION U1(21,25),V1(21,25),U2(21,25),V2(21,25)
      DATA IM,JM/21,25/
C
C     SET DEFAULT VALUES
C
      DATA LUN1,LUN2,LUN3,LUN4,LUN5,LUN6 /11,12,13,14,15,16/
C
      DATA JGRID, IUSOUT, IDOT, NHI
     1    /  10 ,     1  ,  0  ,  -1/
C
      DATA PRESIN, TEMPIN, WINDIN, OTHRIN
     1    /   4. ,    1. ,   400.,    0. /
C
      DATA PDIFIN, TDIFIN, WDIFIN, ODIFIN
     1    /   2. ,   1.  ,  200. ,   0.  /
C
      DATA VECMIN, VECMAX, VDIFMN, VDIFMX
     1    /   0. ,  2000.,   1.  ,  500. /
C
C     **********  END OF USER DEFINED SECTION  **********
?
```

Figure 7. Data statements in PLOTGRD.

TDIFIN . . . . The interval for contouring the difference of two temperature fields. Default is 1.0°C.

WDIFIN . . . . The interval for contouring isotachs of the difference of two vector fields. Default is 200.0 cm sec^{-1}.

ODIFIN . . . . The interval for contouring differences of other types of data. The default is 1.0.

Any of these eight contour intervals can be set to zero, as are OTHRIN and ODIFIN. If this is done, the NCAR routines select an appropriate interval.

Parameters for the wind vector (arrow) plots are:

VECMIN. . . . .The smallest vector magnitude to be drawn. Default is 0.0.

VECMAX. . . . .The largest vector magnitude to be drawn. The plot is scaled so that an arrow of this length will just reach from one data point to the next. Default is 2000.0 cm sec.$^{-1}$.

VDIFMN. . . . .The smallest vector magnitude to be drawn when the difference of two vector fields is being plotted. Any vector smaller than this will not be plotted. Default is 1.0 cm sec.$^{-1}$.

VDIFM . . . . .The largest vector magnitude to be drawn when the difference of two vector fields is being plotted. Default is 500.0 cm sec.$^{-1}$.

4.7 MAP (Plotting Map Backgrounds)

This program and its SUBMIT file (Fig. 8) create plots of the polar stereographic background used with PLOTGRD. The primary purpose of MAP is to generate working base maps for hand plotting and analyzing meteorological data for later digitization. The one input card is in the same format as the primary card for DECKS. The "PLOTTER=" options are the same as in RPLOT.

```
00100 /JOB
00110 DRAWMAP,T270.
00120 USER,METLIB.
00130 CHARGE,RP)
00140 GET,MAIN=DRAWMAP/UN=METLIB.
00230 GET,MAPPROC/UN=METLIB.
00231 CALL,MAPPROC(PLOTTER=1CCWIDE)
00240 REPLACE,TAPE2=MAP.
00290 /EOR
00300 1,23.,25.,8,11,1
 -END OF FILE-
?
```

Figure 8. SUBMIT file for RMAP for running MAP.

4.8 PLOTW,PLOT2W,PLOT2W2 (Combined Submit Files)

These routines combine RWINDS and RPLOT so that plots of wind fields or differences between wind fields can be made from scalar input (Fig. 9,10,11). Figure 9 shows PLOTW which calculates and plots a given series of wind fields. The data cards correspond to those of RWIND followed by RPLOT. PLOT2W (Fig. 10) reads one set of scalars and creates two wind fields corresponding to two different models. PLOT2W2 (Fig. 11) allows the two wind fields to be calculated from different analyses of data for the same observation time. Figure 12 is a sample session running PLOT2W.

```
00100 /JOB
00110 EXAMPLE,T270,
00120 ACCOUNT(METLIB)
00130 CHARGE(RP )
00140 GET,WINDS/UN=METLIB.
00150 GET(TAPE10=SLP)
00160 GET(TAPE11=SAT)
00170 GET(TAPE12=ASTD)
00180 GET,TAPE13=DPTD.
00190 GET(WSUBLIB/UN=METLIB)
00200 FTN,I=WINDS,R=0,L=0.
00210 LDSET(LIB=WSUBLIB)
00220 LGO.
00230 REPLACE(TAPE14=UFIELD)
00240 REPLACE(TAPE15=VFIELD)
00250 RETURN(TAPE10,TAPE11,TAPE12,TAPE13,TAPE14,TAPE15)
00260 GET,MAIN=PLOTGRD.
00270 GET,TAPE11=SLP.
00280 GET,TAPE12=SAT.
00290 GET,TAPE13=UFIELD.
00300 GET,TAPE14=VFIELD.
00310 REWIND(LGO)
00320 GET(PLTPROC/UN=METLIB)
00330 CALL,PLTPROC(PLOTTER=1TK4010)
00340 REPLACE,TAPE2=EXAMPLT.
00350 /EOR
00360 681101180000104  0.8 30.000
00370 0 0 0 4 0 0
00380 0 0 0 0 1 1
00390 09WIND TEST
 END OF INFORMATION ENCOUNTERED.
/
```

Figure 9. SUBMIT file PLOTW for producing wind-field plots from scalar data.

```
00100 /JOB
00110 EXAMPLE,T270,
00120 ACCOUNT(METLIB)
00130 CHARGE(RP )
00140 GET,WINDS/UN=METLIB.
00150 GET(TAPE10=BSLP/UN=SSDATA)
00160 GET(TAPE11=SAT)
00170 GET(TAPE12=ASTD)
00180 GET,TAPE13=DPTD.
00190 GET(WSUBLIB/UN=METLIB)
00200 FTN,I=WINDS,R=0,L=0.
00210 LDSET(LIB=WSUBLIB)
00220 LGO.
00230 REPLACE(TAPE14=UFIELD)
00240 REPLACE(TAPE15=VFIELD)
00250 REWIND(TAPE10,TAPE11,TAPE12,TAPE13)
00260 RETURN(TAPE14,TAPE15)
00270 LDSET(LIB=WSUBLIB)
00280 LGO.
00290 REPLACE(TAPE14=UFIELD2)
00300 REPLACE(TAPE15=VFIELD2)
00310 REWIND,LGO.
00320 RETURN(TAPE10,TAPE11,TAPE12,TAPE13,TAPE14,TAPE15)
00330 GET(PLTPROC/UN=METLIB)
00340 GET(TAPE11=SLP)
00350 GET(TAPE12=SAT)
00360 GET(TAPE13=UFIELD)
00370 GET(TAPE14=VFIELD)
00380 GET(TAPE15=UFIELD2)
00390 GET(TAPE16=VFIELD2)
00400 GET,MAIN=PLOTGRD.
00410 CALL,PLTPROC(PLOTTER=1TK4010)
00420 REPLACE(TAPE2=EXM2PLT)
00430 /EOR
00440 681101180000102
00450 681101180000103
00460 0 0 0 2 2 3
00470 0 0 0 0 1 1
 END OF INFORMATION ENCOUNTERED.
/
```

Figure 10. SUBMIT file PLOT2W for plotting differences between two model runs initialized by the same input data.

```
00100 /JOB
00110 EXAMPLE,T270,
00120 ACCOUNT(METLIB)
00130 CHARGE(RP )
00140 GET,WINDS/UN=METLIB.
00150 GET(TAPE10=SLP)
00160 GET(TAPE11=SAT)
00170 GET(TAPE12=ASTD)
00180 GET,TAPE13=DPTD.
00190 GET(WSUBLIB/UN=METLIB)
00200 FTN,I=WINDS,R=0,L=0.
00210 LDSET(LIB=WSUBLIB)
00220 LGO.
00230 REPLACE(TAPE14=UFIELD)
00240 REPLACE(TAPE15=VFIELD)
00250 REWIND(TAPE10,TAPE11,TAPE12,TAPE13)
00260 RETURN(TAPE10,TAPE14,TAPE15)
00265 GET(TAPE10=SLP2)
00270 LDSET(LIB=WSUBLIB)
00280 LGO.
00290 REPLACE(TAPE14=UFIELD2)
00300 REPLACE(TAPE15=VFIELD2)
00310 REWIND,LGO.
00320 RETURN(TAPE10,TAPE11,TAPE12,TAPE13,TAPE14,TAPE15)
00330 GET(PLTPROC/UN=METLIB)
00340 GET(TAPE11=SLP)
00350 GET(TAPE12=SAT)
00360 GET(TAPE13=UFIELD)
00370 GET(TAPE14=VFIELD)
00380 GET(TAPE15=UFIELD2)
00390 GET(TAPE16=VFIELD2)
00400 GET,MAIN=PLOTGRD.
00410 CALL,PLTPROC(PLOTTER=1CCNARO)
00420 REPLACE(TAPE2=EXM2PLT)
00430 /EOR
00440 681101180000102
00450 681101180000103
00460 0 0 0 2 2 3
00470 0 0 0 0 1 1
 END OF INFORMATION ENCOUNTERED.
/
```

Figure 11. SUBMIT file PLOT2W2 for plotting differences between wind fields created from different SLP fields.

```
CALL"RATE",1200,0,2
CALL"TERMIN"

 80/07/14. 12.09.23.
N O A A / E R L   6600A  80/07/13.       NOS 1.4 509/508.04
FAMILY:
USER NUMBER: METLIB
PASSWORD
********
TERMINAL:     101, TTY
RECOVER/ CHARGE: CHARGE,RP,********
$CHARGE,RP,8C697160.
/GET,PLOT2W
/USER,PMELTRM
USER,PMELTRM.
/CHARGE,RP,********
ACSR,       2.007UNTS.
/SUBMIT,PLOT2W
 12.10.52.AETACCV
/USER,METLIB
USER,METLIB.
/CHARGE,RP,********
ACSR,       2.050UNTS.
/ENQUIRE,JN=CCV
 AGZYCCV  NOT FOUND.
/GET,EXAMPLT
/LNH,F=EXAMPLT
```

Figure 12. Sample session with PLOT2W.

5. SUBROUTINE DOCUMENTATION

5.1 Introduction

A catalog of subroutines on WSUBLIB is in Figure 13. Consult source listings on WSUBS for calling sequences.

5.2 Interpolation (NTERP)

NTERP is a general subroutine for interpolating values to an arbitrary fractional I-J location from a regular grid-point array. To call NTERP, first determine whether the point is closer than one grid from a boundary, in which case the value is assigned via linear interpolation (i.e. KQUAD=5). For an interior point, biquadratic interpolation is used, which utilizes the values at the 16 surrounding points and is consistent with procedures in use at NMC.

5.3 Location on Subgrid (W3FB00,W3FB01)

W3FB01 calculates the latitude, ϕ, and longitude, λ, from polar stereographic grid locations. The transformation equations are:

$$\lambda = 360° - \text{Tan}^{-1}\left(\frac{XJ}{XI}\right) - 90° + \text{ORIENT}$$

$$\Phi = 90° - 2\text{Tan}^{-1}\left[\frac{XMESHL}{a}\,\frac{\sqrt{(XI)^2+(XJ)^2}}{(1+\sin 60°)}\right]$$

Where XI and XJ are grid coordinates with the origin translated to the north pole and a = 6371.2 km, the mean radius of the earth. XMESHL is the mesh length for the particular model. The orientation angle, ORIENT, is 80° for the PE and 105° for the LFM. This is the west longitude which is parallel to the j axis.

W3FB00 calculates the coordinates on the I-J grid given latitude and longitude by solving the transformation equations:

$$XI = \frac{11888.85}{(XMESHL)}\,\frac{(\cos\Phi)(\cos\alpha)}{(1+\sin\phi)}$$

```
        CATALOG OF WSUBS                FILE      1
 REC    NAME        TYPE              LENGTH     CKSUM      DATE

   1    GEOWIN      TEXT                 736      0006
   2    GRDWD       TEXT                1567      6123
   3    TMWND       TEXT                 650      5741
   4    W3FB00      TEXT                 426      0124
   5    W3FB01      TEXT                 725      3543
   6    EDGE        TEXT                 703      4573
   7    W3FC00      TEXT                 171      6007
   8    W3FC02      TEXT                 224      0004
   9    MODEL2      TEXT                 410      1366
  10    SMOGRD      TEXT                 216      7317
  11    GRID        TEXT                 405      7525
  12    MODEL4      TEXT                 110      7002
  13    FIRST       TEXT                  61      5654
  14    BROWN       TEXT                3025      1625
  15    CARDON      TEXT                2413      7363
  16    NTERP       TEXT                1420      0073

  17    * EOF *           SUM =        16774
 CATALOG COMPLETE.
/+
```

Figure 13. Catalog of subroutines in WSUBS.
WSUBLIB is the library version of WSUBS.

$$XJ = \left(\frac{(11888.85)}{XMESHL}\right) \quad \left(\frac{(\cos\Phi)\ (\sin\alpha)}{1 + \sin\Phi}\right) ,$$

where $\alpha = 360° - (\lambda + 90° - ORIENT)$. The pole location is then subtracted to locate the point on the standard grids.

5.4 Speed and Direction (W3FC02,W3FC00)

W3FC02 computes the speed and direction in the meteorological convention of the wind from grid-oriented vector components. The speed is simply $SQRT(u^2 + v^2)$. The wind direction is found from

$$D = TAN^{-1}\ \frac{XJ}{XI} - TAN^{-1}\ \frac{V}{U}$$

where XI and XJ are defined as in W3FB00. W3FC00 performs the reverse operation.

5.5 Thermal Wind (TMWND)

This subroutine calculates the non-dimensional thermal u and v wind component fields. These calculations are made only if one of models 6-10 is to be used. The vertical gradient of the geostrophic wind in the boundary layer is assumed to depend only on the surface horizontal temperature gradient computed by central differences and the Coriolis parameter:

$$u_T \equiv -\ \frac{g}{f^2\bar{T}}\ \frac{\partial\bar{T}}{\partial y} \qquad\qquad v_T \equiv \frac{g}{f^2\bar{T}}\ \frac{\partial\bar{T}}{\partial x}$$

where g is the gravitational acceleration; f, the Coriolis parameter; and air temperature (SAT) is taken for the boundary layer average temperature, $\bar{T}$, at each grid point.

5.6 GRIDSET (GRIDSET)

GRIDSET reads in IGRID, IFACT, and other parameters and adjusts them according to the degree of interpolation and the grid system used.

5.7 Geostrophic Wind (GEOWIN,EDGE)

The components of the pressure gradient at each point of a grid field are found by central differences, dividing by twice the earth distance between adjacent grid points at that latitude. Both the earth-grid distance and the Coriolis parameter depend on the latitude of the grid point. The density of air is specified as constant.

Subroutine EDGE assigns values to the boundary points from the closest interior points.

5.8 Gradient Wind (GRDWD)

A method of successive approximations is used for computing the gradient wind at each interior point (Endlich, 1961). In GRDWD the geostrophic wind speed and the radius of curvature are calculated at each point. The equation $C = C_g - \frac{C^2}{fr}$ is iterated, where C is the gradient wind speed, C_g is the geostrophic wind speed, and r is the radius of the curvature (negative for a clockwise trajectory). EDGE is called at the end to assign gradient wind values to perimeter points.

5.9 Empirical Constants (MODEL4)

Model 4 currently reduces the gradient wind by a set amount and rotates the direction as specified in the calling program.

5.10 Model 2 (MODEL2)

Model 2 utilizes the vertically integrated equations of motion, as suggested by Mahrt (1975) and by Augstein and Heinricy (1976), to yield a first-order approximation of surface winds from geostrophic winds. The equations are:

$$U = U_o + R_o U_1$$

$$V = V_o + R_o V_1$$

where R_o is the Rossby number ($R_o = V_g (fl)^{-1}$; l is horizontal length scale; $R_o = 0.2$ is assumed by subroutine). The solution without inertia is

$$U_o = (1 + C_D^*)^{-1} (U_g - C_D^* V_g)$$

$$V_o = (1 + C_D^*)^{-1} (V_g + C_D^* U_g)$$

where C_D^* is the nondimensional drag coefficient given by $C_D^* = C_D V_g / fH$ where H is the vertical length scale chosen (1 km) and U_g and V_g are the components of the geostrophic wind. U_1 and V_1 are given by

$$U_1 = L(1+C_D^{*2})^{-3} \left[2C_D^* \frac{\partial U_g}{\partial x} + (C_D^{*2} - 1) \frac{\partial V_g}{\partial x} - 2C_D^{*2} \frac{\partial U_g}{\partial y} + C_D^* (C_D^{*2} - 1) \frac{\partial U_g}{\partial y} \right]$$

$$V_1 = L(1+C_D^{*2})^{-3} \left[(1-C_D^{*2}) \frac{\partial U_g}{\partial x} - 2C_D^* \frac{\partial V_g}{\partial x} + C_D^* (1-C_D^{*2}) \frac{\partial U_g}{\partial y} - 2C_D^{*2} \frac{\partial V_g}{\partial y} \right]$$

where L is twice the mesh length and the partials are in the finite difference form. Another version of MODEL2 specifies H as proportional to u_*/f, where u_* is the friction velocity.

5.11 Models 6-8 (MODEL6, MODEL8, BROWN, CARDON, etc)

Models 6-8 use the magnitude and direction of the thermal wind, the air-sea temperature difference, and the latitude to correct for stability and baroclinicity of the boundary layer in deriving surface-wind speed and inflow angle from the gradient wind. MODEL6 uses the model of R. Brown, summarized in Appendix A. MODEL8 uses the model provided by V. Cardone, summarized in Appendix B.

6. ACKNOWLEDGEMENTS

This report is a contribution to the Marine Services Project at Pacific Marine Environmental Laboratory. Subroutines W3FB00 and W3FB01 and subroutine NTERP are adaptations of subroutines in use at the National Meteorological Center. Our thanks to Clifford M. Fridlind, Matthew H. Hitchman, Steven Ghan and Jon O. Nestor who have contributed to the development of METLIB. T. Liu contributed substantially to Appendix A. V. Cardone provided a copy of the computer program of his boundary layer model. R. Brown was supported in part by the Jet Propulsion Laboratory during preparation of this memorandum.

7. REFERENCES

Augstein, E. and D. Heinricy (1976): Actual and geostrophic wind relationships in an accelerated marine atmospheric boundary layer. Beitrage zur Physik der Atmosphare 49, 55-68.

Cressman, G. (1959): An Operational Objective Analysis System. Mon. Wea. Rev., 87, 367-374.

Endlich, R.M. (1961): Computation and Uses of Gradient Winds. Mon. Wea. Rev., 89, 187-191.

Flattery, T.W. (1970): Spectral models for global analysis and forecasting. Proceedings, Sixth AWS Technical Exchange Conference, AWS Tech. Rept., 242, Scott AFB, Ill., 42-54.

Holl, M., and B. Mendenhall (1971): FIB-fields by information blending. Final report to Commanding Officer, Fleet Numerical Weather Central, Project M-167, 66 pp.

Jenne, R. L. (1975): Data sets for meteorological research. NCAR Tech. Note NCAR-TN/1A-111, 194 pp.

Mahrt, L. (1975): The influence of momentum advections on a well mixed layer, Quart. J. R. Met. Soc., 101, 1-11.

Wright, T. (1977): NCAR graphics software. NCAR Technical Note, Preliminary Edition.

Appendix A: DERIVATION OF THE UNIVERSITY OF WASHINGTON (BROWN) PLANETARY BOUNDARY LAYER MODEL

1. SOLUTION FOR THE PBL WITH NEUTRAL STABILITY

An appropriate set of non-dimensionalized equations for a non-accelerating lower atmosphere is

$$V + E^2 (KU_z)_z - P_x/\rho = 0 \qquad (1)$$

$$U - E^2 (KV_z)_z + P_y/\rho = 0 \qquad (2)$$

where E is an Ekman number defined by $E = \delta/H$, with $\delta^2 = 2\bar{K}/f$; H is an arbitrary scale height; f is the Coriolis parameter; K is an eddy coefficient, $\bar{K}$ is its mean; V_o is the characteristic velocity scale; $z = \hat{z}/H$; $V = \hat{V}/V_o$. Hats denote dimensional variables while characteristic values are always dimensional: u_*, G, δ, z_o, ρ_o, T_o, and L. All other terms use standard notation. A continuous solution for the domain $0 \leqq z \leqq \infty$ can be obtained by considering three scale heights H and the appropriate solution for each regime is given in Table 1.

Table 1: Flow Solutions for Scale Heights H above the Surface

H	E	Equations	Solutions
$\to\infty$	$\to 0$	$\underset{\sim}{V} + \nabla P/\rho = 0$	Geostrophic (w/corrections)
$0[\delta]$	0[1]	(1&2) with E= 1	Ekman/Taylor layer (3)
		K = constant	$\frac{\hat{U}}{G} = \cos\alpha - e^{-\zeta}[\cos(\alpha-\zeta) - \frac{\hat{U}_o}{G}\cos\zeta]$
		$V_o \equiv G$	$\frac{\hat{V}}{G} = \sin\alpha + e^{-\zeta}[\sin(\alpha-\zeta) - \frac{\hat{U}_o}{G}\sin\zeta]$
			$\underset{\sim}{\hat{U}} \to G$ at $\zeta \to \infty$
			$\underset{\sim}{U} \to \underset{\sim}{U}_o$ at $\zeta \to 0$

Cont.

Table 1: Flow Solutions for Scale Heights H above the Surface (continued)

H	E	Equations	Solutions
			$\zeta \equiv \hat{z}/\delta$
			α is angle between $\underset{\sim}{V}_g$ and $\underset{\sim}{U}_o$
			Surface Layer
$0[z_o]$	∞	$(KU_z)_z = 0$	$\hat{U} = \frac{u_*}{k} \ln \frac{\hat{z}}{z_o}$ (4)
			$K = ku_* \hat{z}$, $K_o = ku_* z_o$
			$u_* = (\tau_o/\rho_o)^{\frac{1}{2}} = V_o$

where τ_o, ρ_o, K_o and z_o are stress, density, eddy viscosity and height (roughness scale) at U = 0.

The velocity V_o can be related to the turning angle, α, using Taylor's lower boundary condition that near the surface, the velocity and stress are in the same direction.

$$\hat{U}_o = G(\cos \alpha - \sin \alpha) \tag{5}$$

With equations 3, 4, and 5, velocity profiles can be calculated through the PBL provided that: u_* and z_o are known for the surface layer; either h_p, the height of the surface layer, or α, the turning angle between G and u_*, is known; and G and δ are known for the outer layer. By examining the matching requirements for the two-layer solution, the need for h_p and δ will be reduced to only the need for the ratio $h_p/\delta = \lambda$.

When the velocity, shear and eddy viscosity in the surface layer and the Ekman/Taylor layer are matched, one obtains

$$kG/u_* \sin \alpha = -B$$
$$kG/u_* \cos \alpha = -A', \tag{6}$$

where A' and B are similarity parameters which depend on the single similarity parameter, λ. So,

$$u_*/G = k(B^2 + A'^2)^{-\frac{1}{2}} \tag{7}$$

$$B = e^{\lambda}/(2\lambda\cos\lambda)$$

$$A' = -\ln \lambda E_s - (\cos \lambda - \sin \lambda)/(2\lambda \cos \lambda) \tag{8}$$

with $E_s = \delta/z_o$, $\delta = 2k\lambda u_*/f$.

The solution is completed by adding an empirical relation for z_o as a function of u_* and assigning values to the similarity parameter, λ.

There exist several choices for $z_o(u_*)$. We have examined several possibilities and have chosen the empirical relation from Kondo (1975) (see Section IX) for use in the model. An iterative solution for u_* is needed.

2. THE NEUTRAL PBL WITH SECONDARY FLOW IN THE EKMAN/TAYLOR LAYER

It has been shown that the first-order closure (K-theory) solution for the Ekman/Taylor layer is unstable to infinitesimal perturbations and therefore doesn't exist (see, e.g., Brown, 1974). There is a non-linear equilibrium finite perturbation solution (Brown, 1970) and this correction has been incorporated in the model. The basic mean flow is altered such that $(U,V,W) = (U_E,V_E) + (U_2,V_2) + (u_2,v_2,w_2)$ where (U_E,V_E) is the solution of the homogeneous equation (3), (U_2,V_2) are the mean flow modifications, and (u_2,v_2,w_2) are the zero mean secondary flow. The finite perturbation modifies the basic Ekman/Taylor equation (3) with a forcing function depending on $\overline{w_2 v_2}_z$ on the right-hand side of the second equation.

The amended equations for u_* is

$$\frac{u_*}{kG} = \frac{-\gamma A' - \beta B + [A'^2 + B^2 - (\gamma B - \beta A')^2]^{\frac{1}{2}}}{A'^2 + B^2} \tag{9}$$

$$\frac{kG}{u_*}(\sin\alpha+\beta) = -B \tag{10}$$

$$\frac{kG}{u_*}(\cos\alpha+\gamma) = -A' \qquad (11)$$

where $$\beta = \frac{-e^{\lambda}}{2\cos\lambda} U_{2_\zeta}(\lambda)$$

$$\gamma = \frac{\cos\lambda - \sin\lambda}{2\cos\lambda} U_{2_\zeta} + U_2$$

evaluated at $\zeta = \lambda$.

The neutral value of U_2 is given in Brown (1970).

3. THE MODIFIED EKMAN/TAYLOR LAYER WITH THERMAL WIND

When thermal wind is added to the model, the pressure gradient term in (1) and (2) becomes a function of (T_x, T_y), and, under the approximation that the temperature gradient is constant with height,

$$P_x/\rho = (P_x/\rho)_{z=0} + (g/T_0)\hat{T}_{\hat{x}}\hat{z}.$$

The equation for the geostrophic balance throughout the layer may be written

$$(U_g,V_g) = (U_{go},V_{go}) + (u_T,v_T)\,\zeta$$

$$(u_T,v_T) = \frac{g}{fT_o}(-T_y,T_x),\quad (U_{go},V_{go}) = (\cos\alpha,\ \sin\alpha).$$

The thermal wind must be added to (3) and the equations for β and γ become:

$$\beta = \frac{-e^{\lambda}}{2\cos\lambda}\left[u_T - \frac{\cos\lambda + \sin\lambda}{e^{\lambda}} v_T + U_{2_\zeta}\right]_{\zeta=\lambda}$$

$$\gamma = \left\{\left[\frac{\cos\lambda - \sin\lambda}{2\cos\lambda} + \lambda\right] u_T + \left\{\frac{1}{2e^{\lambda}\cos\lambda}\right\} v_T + U_2 + \frac{\cos\lambda - \sin\lambda}{2\cos\lambda} U_{2_\zeta}\right\}_{\zeta=\lambda}$$

while (9) remains the fundamental equation for $u_*(G)$.

4. THE STRATIFIED PBL

Variation in the bulk stratification of the PBL has an effect on the surface-layer solution and upon the modified Ekman/Taylor-layer solution. The former effect has been empirically parameterized (Section 10) and (4) becomes

$$U = u_* \, [\ln(z/z_o) - \psi]/k, \tag{12}$$

where ψ is an empirical correction which depends on $\hat{z}/L$; L is the Obukhov scale = $-Tu_*^2/(gkT_*)$; $T_* = -(\text{heat flux})/(\rho C_p u_*)$. An iteration on the stratification correction is necessary since it depends upon u_*. The equations for A', B and δ are

$$B = \frac{e^{\lambda}}{2\,\lambda\cos\lambda}\left[1 - \lambda\psi_\zeta\right]\zeta=\lambda \tag{13}$$

$$A' = -\left[\ln \lambda E_s + \frac{\cos\lambda - \sin\lambda}{2\,\lambda\cos\lambda}\right] - \left[\psi + \frac{\cos\lambda - \sin\lambda}{2\cos\lambda}\,\psi_\zeta\right]\zeta=\lambda$$

$$\delta = 2k\lambda u_*/[f(1-\lambda\psi_\zeta)].$$

The stratification effect on the outer layer appears in U_2/G. This is fairly strong and nearly constant in unstable stratification and decreases to zero when the Richardson number approaches 1/4. This stratification effect can be empirically related to a stratification parameter $\mu = ku_*/(fL)$ from the magnitude calculations by Brown (1972):

$$\begin{aligned}
&U_2(\lambda) = 0.05 && \mu \leq 0 \\
&U_{2\zeta}(\lambda) = 0.1 && \\
&U_2(\lambda) = 0.05\,(\mu_{max} - \mu)/\mu_{max} && 0 \leq \mu \leq \mu_{max}\ (Ri = 0.25) \\
&U_{2\zeta}(\lambda) = 0.1\,(\mu_{max} - \mu)/\mu_{max} && \\
&U_2 = U_2\zeta = 0 && \mu \geq \mu_{max}
\end{aligned} \tag{14}$$

5. HUMIDITY AND THE MOLECULAR SUBLAYER

In a marine atmosphere, the humidity can significantly change the buoyancy of the air since moist air is lighter than dry air. The model uses the relative humidity of the air to evaluate this term. To include this effect, the Obukhov length is defined as

$$L = -T_v u_*^2/(gkT_{v*}),$$

where $T_v = T(1 + 0.61Q)$, $T_{v*} = T_*(1 - 0.61Q) + 0.61TQ_*$, $T_* = -H_o/(c_\rho u_*)$, $Q_* = -E_o/(\rho u_*)$, T is the potential temperature, Q is the specific humidity, H_o and E_o are the heat and moisture fluxes.

In order to determine L, the heat and moisture fluxes are determined with the diabatic profiles

$$\begin{aligned}(T-T_s)/T_* &= (\ln(z/z_T) - \alpha_T)(K_{H_o})^{-1} \\ (Q-Q_s)/Q_* &= (\ln(z/z_Q) - \alpha_Q)(K_{E_o})^{-1},\end{aligned} \tag{15}$$

where $\alpha_T = K_{H_o}/K_{M_o}$ and $\alpha_Q = K_{E_o}/K_{M_o}$ are the ratios of turbulent diffusivities at neutral conditions. These profiles, however, are not valid close to the interface. While transport in air and water is facilitated by turbulent motion, the motion is suppressed near the interface and one expects molecular diffusion to dominate. Since diffusion is a much slower process in the regions on both sides of the interface, there is a reduction in exchanges between the ocean and the atmosphere. Most of the variation in velocity, temperature, and passive variable concentration in the lower part of the atmosphere and upper part of the ocean are found in these regions, which will be referred to as the interfacial sublayers. The lower boundary values z_T and z_Q in (15) depend on the temperature and moisture distributions in the sublayer in the air. Liu and Businger (1975) derived sublayer profiles based on the assumption of intermittent instability. The values of z_T and z_Q are determined by matching the sublayer profiles with (15) (Liu et al., 1979). Their values can be approximated by

$$\begin{aligned}z_T u^*/\nu &= a_1 Rr^{b_1} \\ z_Q u_*/\nu &= a_2 Rr^{b_2},\end{aligned} \tag{16}$$

where ν is the kinematic viscosity. The values of a_1, a_2, b_1, b_2, for ranges of the roughness Reynolds number $Rr = zU/\nu$ are shown in Table 2.

Table 2: The Lower Boundary Values of the Logarithmic Profiles

$R_T = a_1 Rr^{b_1}$	$R_Q = a_2 Rr^{b_2}$	$Z_T u_*/\nu = a_1 Rr^{b_1}$		$Z_Q u_*/\nu = a_2 Rr^{b_2}$
Rr	a_1	b_1	a_2	b_2
0-0.11	0.177	0	0.292	0
0.11-0.826	1.376	0.929	1.808	0.826
0.925-3.0	1.026	-0.599	1.393	-0.528
3.0-10.0	1.625	-1.018	1.956	-0.870
10.0-30.0	4.661	-1.475	4.994	-1.297
30.0-100.0	34.904	-2.067	30.790	-1.845

6. MODEL SUMMARY

The University of Washington Planetary Boundary Layer (PBL) model is a composite which includes:

1) A surface layer with no turning of the wind and a velocity which increases logarithmically with height. The log profile is corrected for variable stratification using the Businger/Dyer model (Section 10). It is also corrected for variable humidity and diabatic effects in the interfacial layer.

2) An outer layer model in which velocity turning takes place from the top of the surface layer to the upper boundary flow condition--the free stream or geostrophic flow. This Ekman/Taylor layer flow is corrected for stratification effects directly through the variable secondary flows from Brown (1970) and for thermal wind.

3) A similarity relationship derived from matching the two layers. This involves the geostrophic flow G, the Ekman depth $\delta = (2K/f)^{\frac{1}{2}}$, the friction velocity, u_*, and the surface roughness scale, z_o, in an equation relating the geostrophic drag coefficient, u_*/G, to the similarity parameter, $\lambda = h_p/\delta$.

4) An assumed relation between z_o and u_* taken from Kondo (1975) (Section 9).

The basic equations are:

Surface layer:

$$\hat{u}/u_* = [\ln \hat{z}/z_o - \psi(\hat{z}/L)]/k,$$

where ψ is determined empirically from the Businger and Dyer method (Section 10) and

$$L = \frac{-Tu_*^2}{kgT_*} \qquad T_* = \frac{T_a - T_s}{\alpha k(\ln \frac{h_*}{z_o^*} - \psi)}$$

and h_* and z_o^* are obtained from Liu's (1978) correction for the interfacial layer, allowing for humidity effects.

Ekman/Taylor layer:

$$U = \cos\alpha + u_t\zeta - e^{-\zeta}[(\cos\zeta - \sin\zeta)\sin\alpha + v_t\cos\zeta] + U_2$$

$$V = \sin\alpha + v_t\zeta - e^{-\zeta}[(\cos\zeta + \sin\zeta)\sin\alpha + v_t\sin\zeta] + V_2$$

$$(U_g, V_g) = (\cos\alpha, \sin\alpha) + (u_t, v_t)$$

$$(u_T, v_T) = g\delta/(fGT_o)(-\hat{T}_{\hat{y}}, \hat{T}_{\hat{x}}) \text{ and } \alpha < \underset{\sim}{u}_*, \underset{\sim}{V}_g >$$

$(\hat{U}_2, \hat{V}_2)/G$ are parameterized from the results of Brown (1972).

Applying the Matching Condition gives the system:

$$\frac{kG}{u_*}(\sin\alpha + \beta) = -B$$

$$\frac{kG}{u_*}(\cos\alpha + \gamma) = -A'$$

$$u_* = kG\ \frac{-\gamma A' - \beta B + [A'^2 + B^2 - (\gamma B - \beta A')^2]^{\frac{1}{2}}}{A'^2 + B^2}$$

$$B = \frac{e^{\lambda}}{2\lambda\cos\lambda}\left[1 - \lambda\psi_{\zeta}(HL)\right]$$

$$A' = -1n\lambda E_s + \psi(HL) - \frac{\cos\lambda - \sin\lambda}{e^{\lambda}}B$$

$$E_s = \delta/z_o = 2k\lambda u_*/[fz_o(1 - \psi_{\zeta}(HL)];\ HL = \frac{\lambda\delta}{L}$$

$$\beta = \frac{e^{\lambda}}{2\cos\lambda}\left[-u_T(\lambda) + \frac{\cos\lambda + \sin\lambda}{e^{\lambda}}v_T(\lambda) - U_{2_{\zeta}}(\lambda)\right]$$

$$\gamma = \lambda u_T(\lambda) + \frac{\cos\lambda}{e^{\lambda}}v_T(\lambda) + U_2(\lambda) - \frac{\cos\lambda - \sin\lambda}{e^{\lambda}}\beta.$$

The roughness parameter, $z_o(u_*)$, is specified per Kondo (1975) and Liu (Section 9), $\lambda = 0.15$ from Brown (1978), and $U_2(\lambda)$ from Brown (1972). The value of L requires air-sea temperature differences and Businger/Dyer corrections (Section 10). The thermal wind ($\underset{\sim}{u}_T$) requires horizontal temperature gradients.

7. PROGRAM FLOW DIAGRAM

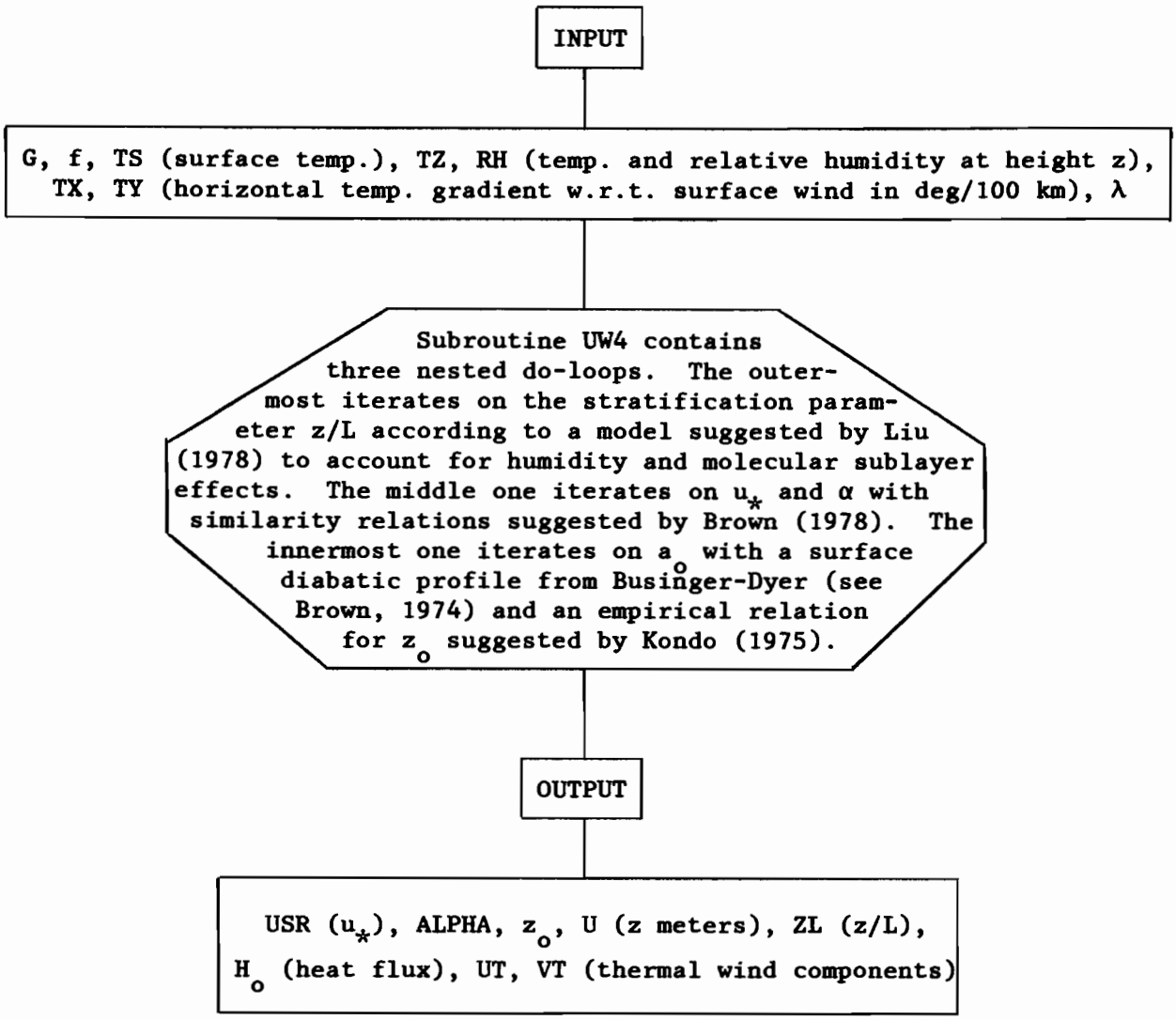

8. MODEL SENSITIVITY

The model is based upon the ψ formulation of Businger-Dyer and the Kondo (1975) $z_o(u_*)$ relation. Other aspects which differ from previous models are: the inclusion of equilibrium producing secondary flow in the outer layer; adding a molecular sublayer and relative humidity effect; and adding a thermal wind. The importance of each of these terms has been investigated by varying the basic parameters and checking output variations for representative cases.

Some changes due to secondary flow are shown in Table 3.

Table 3: Secondary Flow Effect (Neutral)

G m sec^{-1}	U_2	U_{2_z}	z_o cm	U_{10} ms^{-1}	u_* cm sec^{-1}	α deg.
10	0	0	.017	7.0	25	15
10	-0.05	0.1	.020	7.6	28	12

The variation of the surface roughness parameter z_o and the PBL height parameter, δ, with G is shown in Figure 1. Both increase nearly linearly with freestream flow magnitude.

The default relative humidity is 0.7. The effect of humidity is shown in Figure 2. There is a change in stratification over the range of humidity, greatest in slightly stable regimes. The effect on δ is shown, amounting to a 50 percent change near neutral stratification.

The effects of thermal wind on the model are shown in Figure 3. Variation of u_* and α with T_x (temperature gradient in the U_{10} direction, $T_y \equiv 0$) and with $T_y (T_x \equiv 0)$ are shown in Figure 3a. The effect of direction is shown in 3b, where a constant $\nabla T \cong 4.0$ is rotated. This is a large thermal wind and the effect is significant. For $\nabla T \leqq 2°/100$ km, the u_* error is $\leqq 10$ percent, and α may change by $\leqq 5°$.

From the matching of K at the patching height;

$$\delta = 2k\lambda u_*/[f(1-\lambda\psi_z)].$$

Using Ekman's approximate boundary layer height, $H = \pi\delta$, this becomes:

$$\frac{Hf}{u_*} = 2\pi k\lambda/(1-\lambda\psi_z).$$

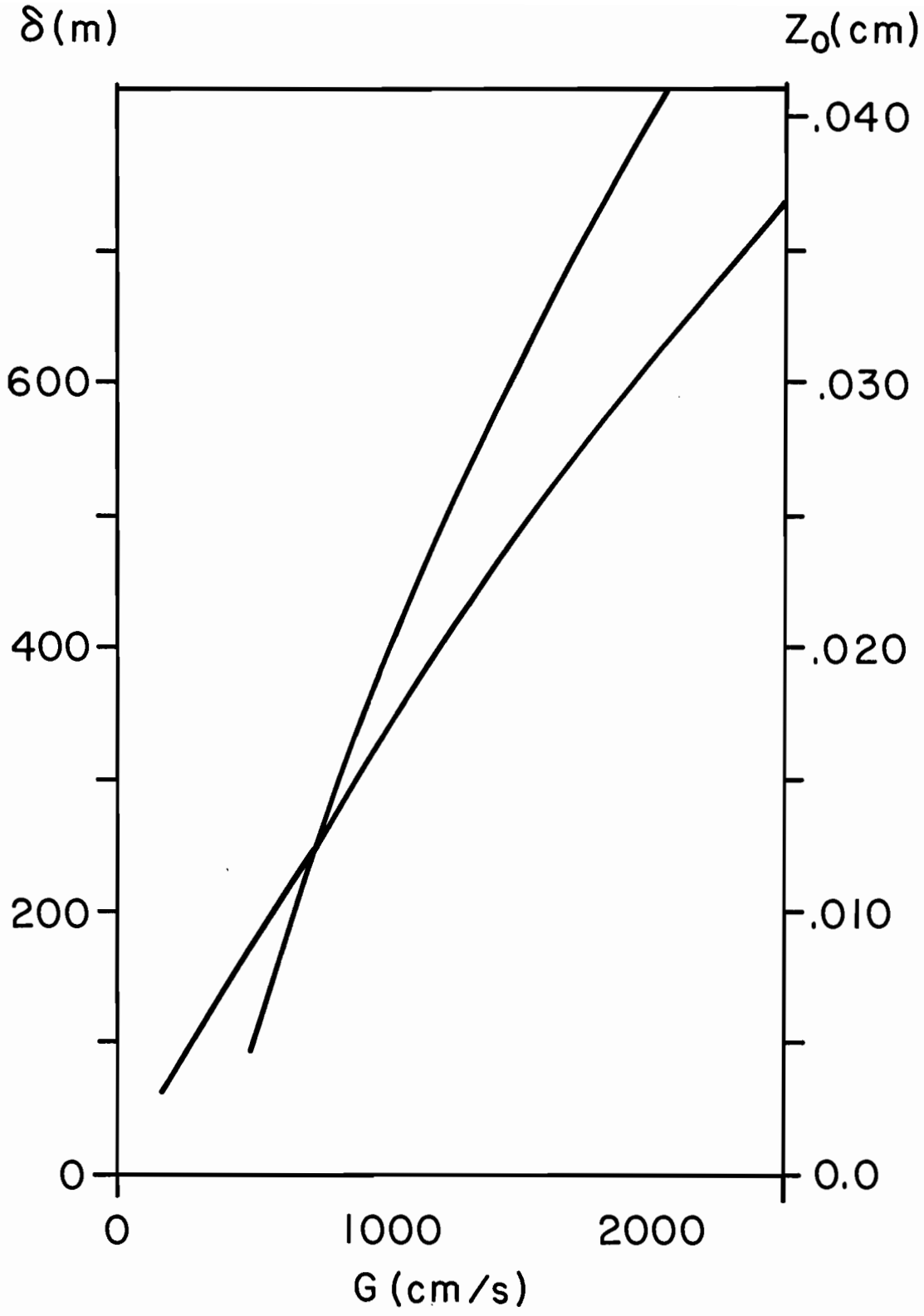

Figure 1 -- Roughness parameter z_o and depth of frictional resistance δ versus geostrophic flow G (at 45° lat., RH = 0.7, neutral stratification), u_*/G is approximately constant 0.028.

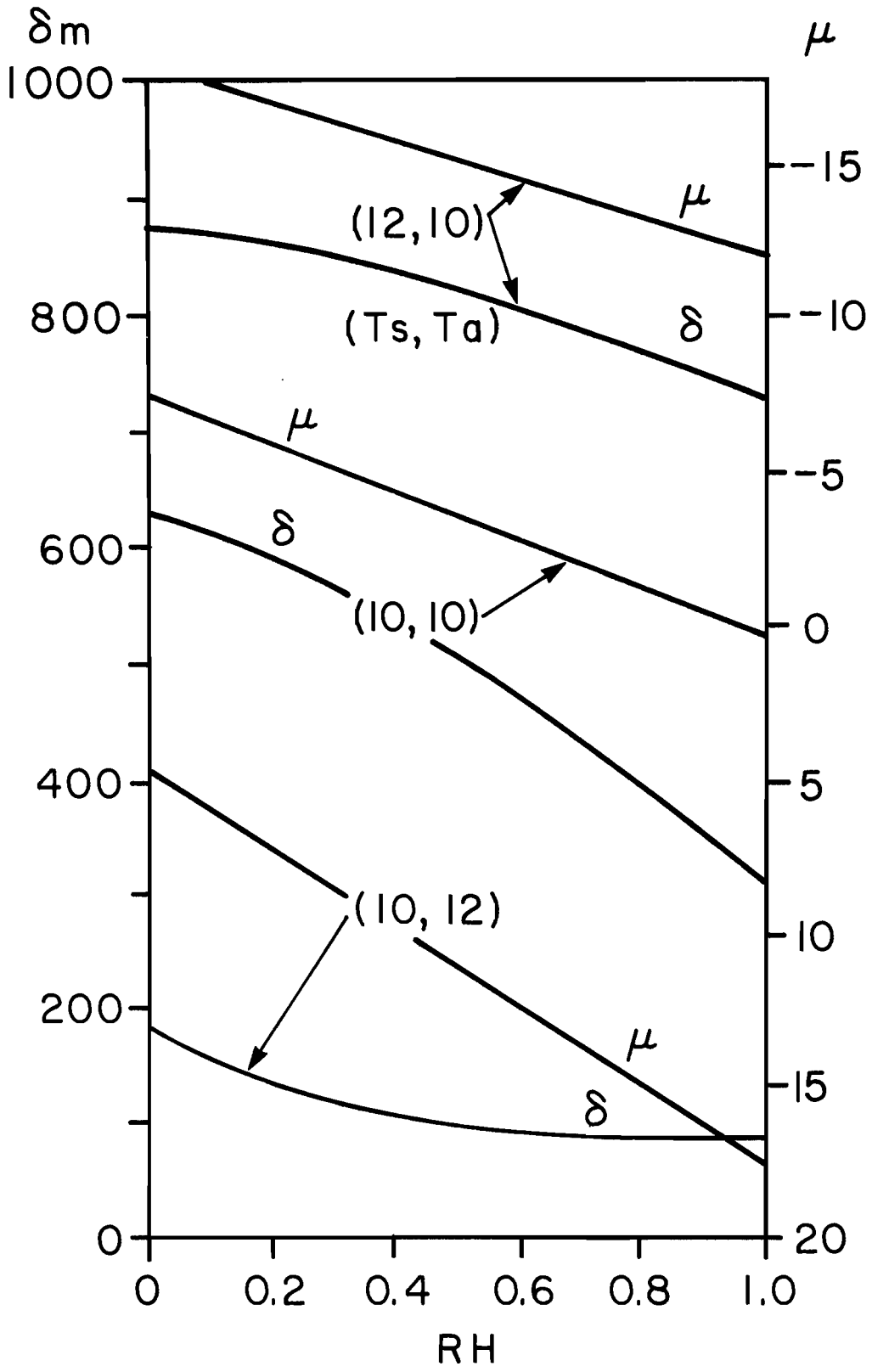

Figure 2 -- u_*, z_o and δ versus relative humidity at stable (T_s= 10, T_z = 12), near neutral (T_s = T_z= 10) and unstable (T_s = 12, T_z = 10) stratification (at 45° lat., G = 10 m s^{-1}).

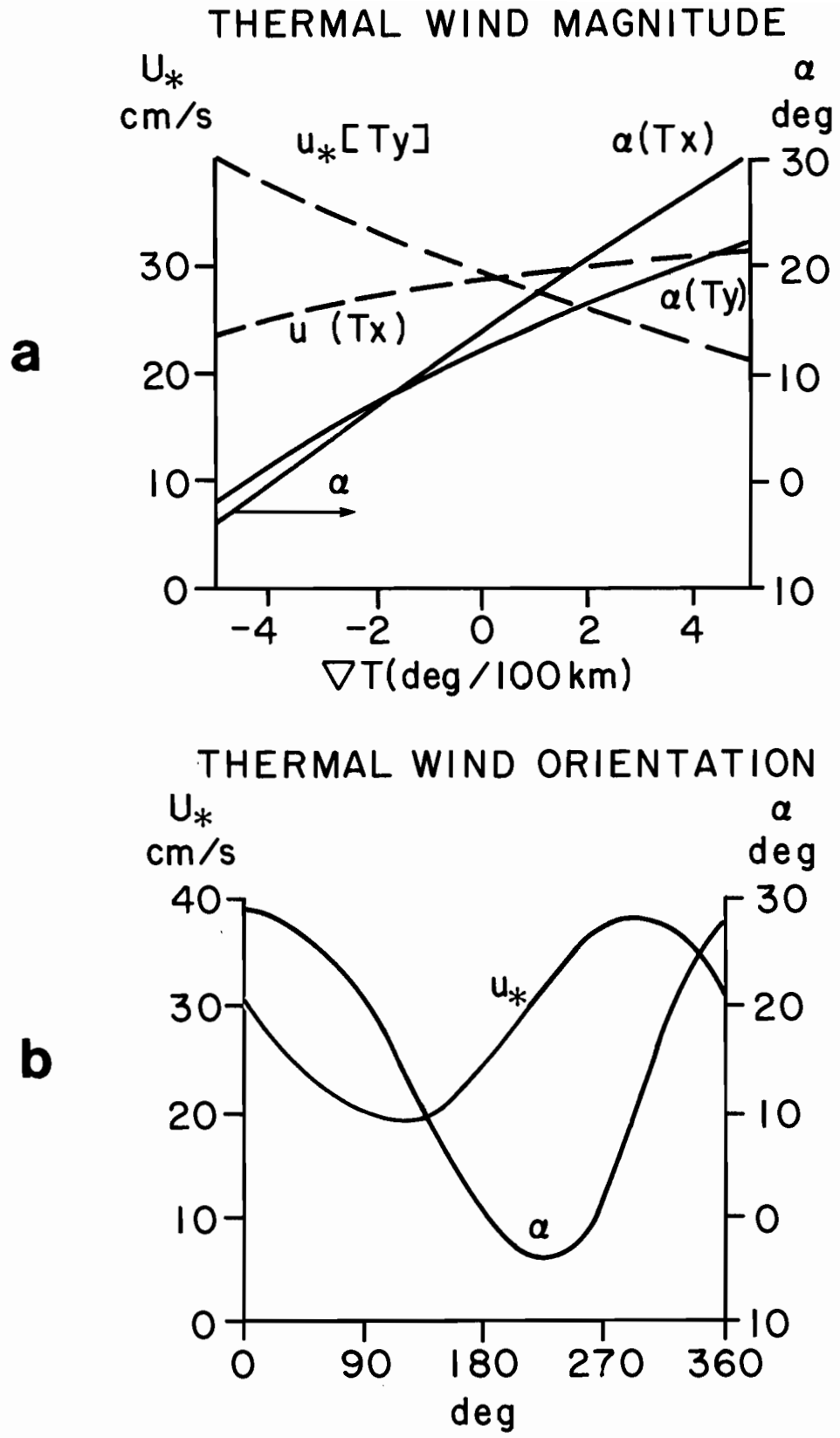

Figure 3 -- u_*/G and α (geostrophic departure) versus temperature gradient for variable gradient parallel to surface flow ($T_y = 0$), normal to surface flow ($T_x = 0$) and for constant gradient ($\nabla T = 4$) at various angles to U_{10} (at 45° lat., RH = 0.7, G = 10 m s^{-1}, neutral).

From Paulson's (1970) empirical expression for $\Psi(\hat{z}/L)$, model results for PBL height variation with stratification are shown in Figure 4.

The height of the PBL in stably stratified conditions has often been written:

$$\frac{Hf}{u_*} = a\mu^{-\frac{1}{2}}, \tag{17}$$

where $\mu = u_*/fL$ and "a" has been found to be from 0.7 to 2, generally assumed to be near unity. With $\Psi = -a_o\hat{z}/L$ in stable stratification,

$$\frac{Hf}{u_*} = \frac{2\pi k\lambda}{1 - \frac{a_o\lambda\mu}{k\pi}\frac{Hf}{u_*}}$$

$$\frac{Hf}{u_*} = \frac{1 \pm (1 - 8a_o\lambda 2\mu)^{\frac{1}{2}}}{\frac{2a_o\lambda}{k\pi}\mu}$$

$$\frac{Hf}{u_*} = [(1+0.84\mu)^{\frac{1}{2}} - 1]/(1.1\mu) \tag{18}$$

when $a_o = -4.7$, $k = 0.4$, and $\lambda = 0.15$

In case of large μ, (18) is approximated by 17 with $a = 0.8$.

While the curve fit (17) breaks down at $\mu = 0$, (18) has no such problem, as shown in Figure 4.

Figure 5 shows the effects of stratification on u_*, U_{10}, $U_{19.5}$ and α. Stable stratification has a large effect, and small changes near neutral result in large change in α and u_*. The decreased effect on $U_{19.5}$ and U_{10} compared to u_* is evident, a result of the higher level flow being more influenced by the constant upper boundary condition, G = constant and less by the layer stratification.

9. THE NEUTRAL DRAG COEFFICIENT AND ROUGHNESS PARAMETER

Under neutral conditions, the wind speed at height z in the atmospheric surface layer is given by

$$(\hat{U} - \hat{U}_s)/u_* = \ln(\hat{z}/z_o)/k, \tag{19}$$

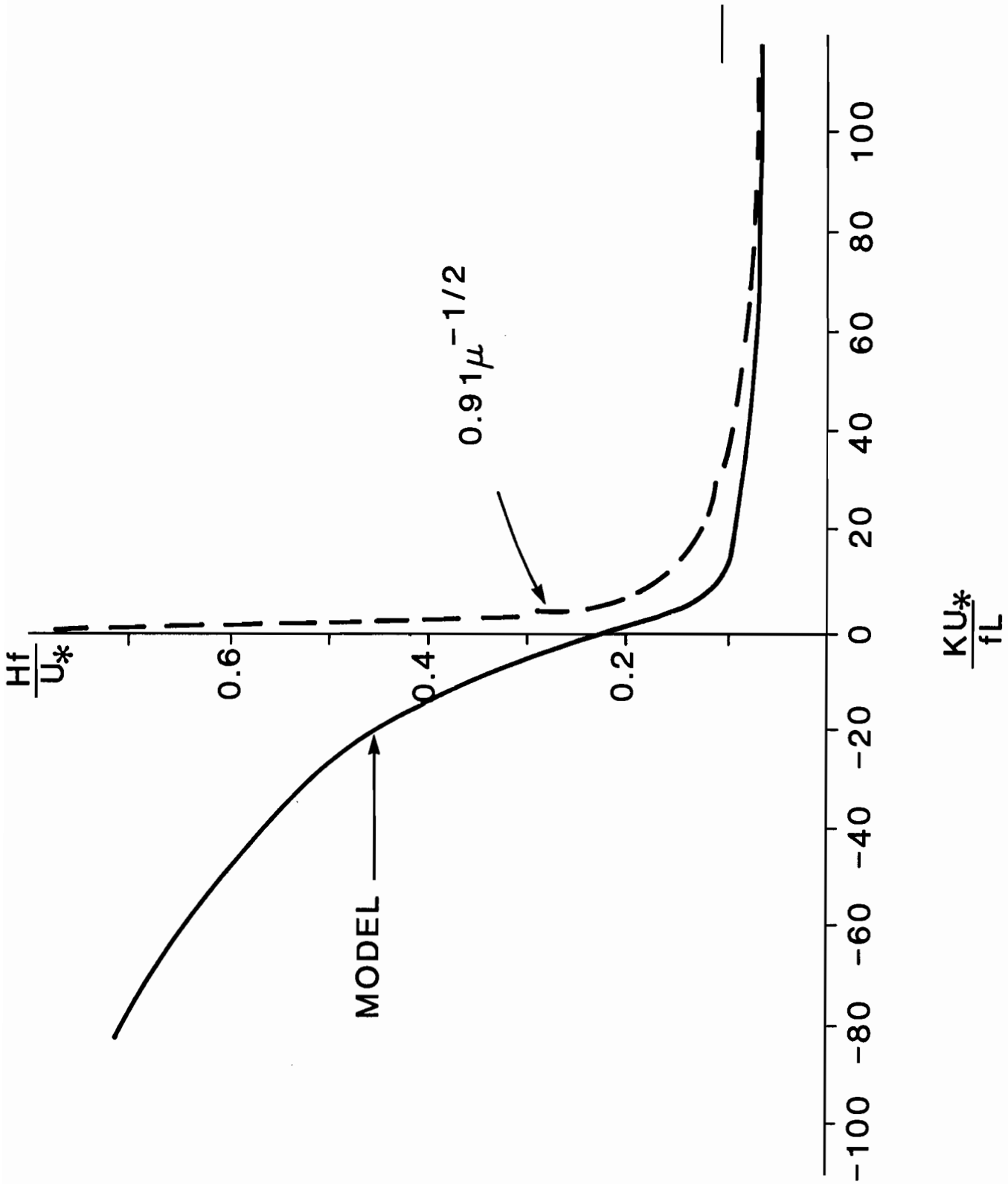

Figure 4 -- The PBL height from the model versus stratification (solid line). The dashed line is the approximate relation $H = 0.9\ \mu^{-\frac{1}{2}}$, RH = 0.7, G = 10 m sec^{-1}, lat. = 45° and $H \sim \pi\delta$.

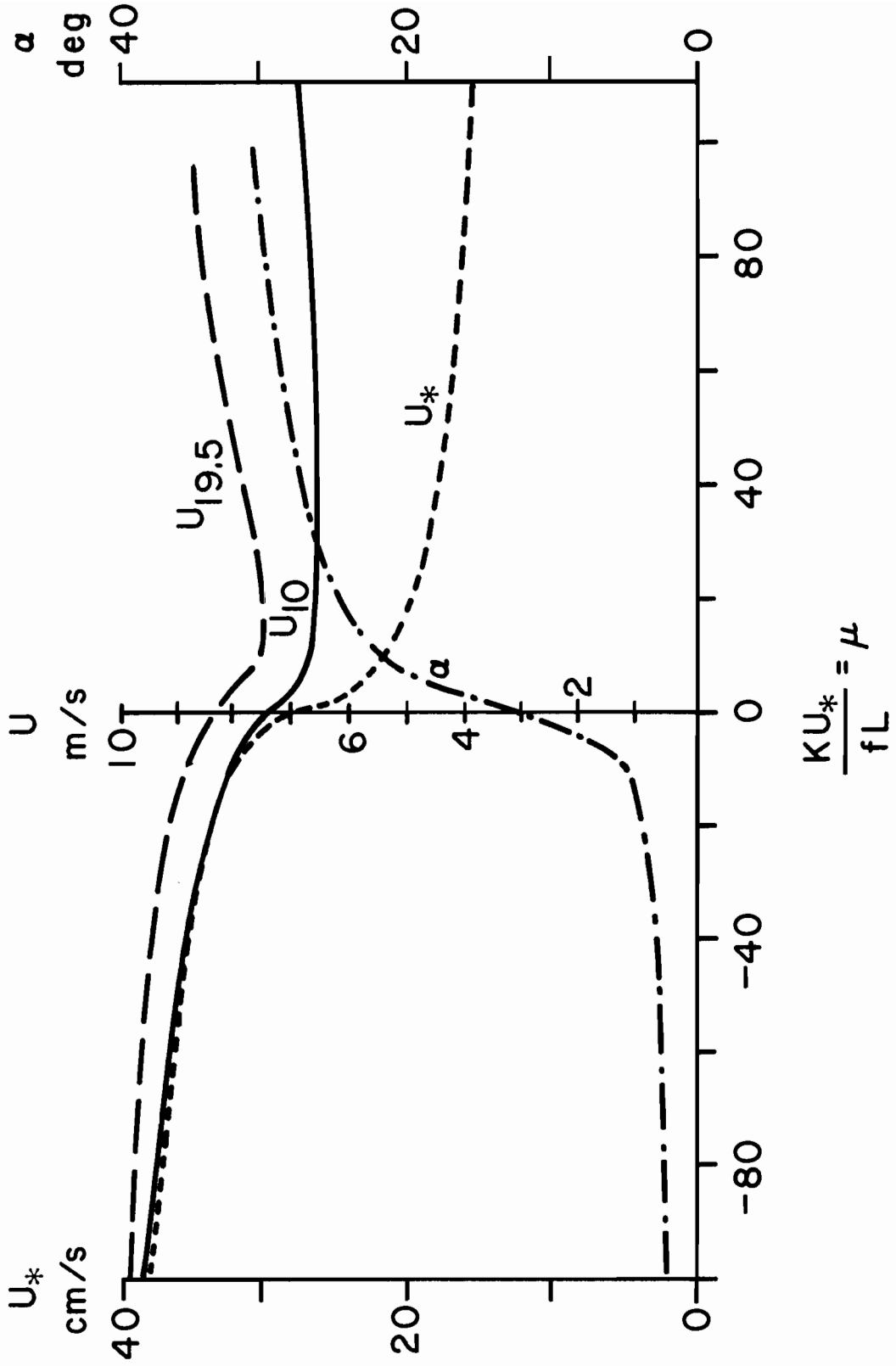

Figure 5 -- $U_{19.5}$, U_{10}, u_* and α versus stratification. RH = 0.7, lat. = 45°, G = 10 m s^{-1}.

where U_s is the surface drift. The drag coefficient, C_D, relates wind to stress:

$$\tau/\rho = C_D(\hat{U} - \hat{U}_s)^2. \tag{20}$$

By combining (19) and (20), a relation between z_o and C_D can be determined:

$$z_o = z_{exp}(-k/C_D^{\frac{1}{2}}). \tag{21}$$

The reference height for C_D is generally taken to 10 m.

Both the measurements of Nikuradse (1933) on pipe flow and those of Kondo (1973) at an air-sea interface indicate:

$$z_o = G_1 \nu/u_* \qquad \text{for } \xi u_*/\nu \leq r_1 \tag{22a}$$

$$z_o = f(\xi u_*/\nu) \qquad \text{for } r_1 \leq \xi u_*/\nu \leq r_2 \tag{22b}$$

$$z_o = G_2 \xi \qquad \text{for } r_2 \leq \xi u_*/\nu . \tag{22c}$$

Nikuradse (1933) defined ξ as the actual mean diameter of the sand grains used as roughness elements and found $r_1 = 5$, $r_2 = 70$, $G_1 = 0.11$ and $G_2 = 0.03$. Kondo (1973) defined ξ as the root-mean square waveheight for frequencies between 20 and 200 rad/sec^{-1} and found $r_1 = 5.7$, $r_2 = 67$, $G_1 = 0.11$ and $G_2 = 0.07$. These results separate the flow roughly into smooth, transition and rough regimes.

For a fully rough air-sea interface, Charnock (1955) obtained by dimensional reasoning

$$z_o = \frac{a u_*^2}{g} , \tag{23}$$

where g is the acceleration due to gravity and a is a universal constant. Wu (1969) found that for $U_{10} < 3$ m s^{-1}, (22a) is valid; for 3 m s^{-1} $< U_{10} < 15$ m s^{-1}, (23) is valid; and for $U_{10} \geq 15$ m s^{-1}, z_o is a constant.

Recently, a number of investigators have obtained empirical relations between C_D and U_{10}. Smith and Banke (1975) correlate C_D and U_{10} for 111 data runs and obtained

$$10\ C_D = 0.63 + 0.066\ U_{10} \tag{24a}$$

for U_{10} between 3 and 21 m s^{-1} Garrett (1977) obtained from 18 sets of data including those of Smith and Banke (1975)

$$10\ C_D = 0.75 + 0.067\ U_{10} \tag{24b}$$

for U_{10} between 4 and 21 m s^{-1}. Both (24a) and (24b) agree with (23). Kondo (1975), by using wind-wave data from Kondo et al. (1973), obtained approximate relations in the form:

$$10^3 C_D = p + qU^r_{10} \tag{24c}$$

that agree with (22). The values of p, q, r for different ranges of wind speed are shown in Table 4. The difference between C_D given by (24a), (24b) and (24c) are small for moderate wind speeds. Garratt (1977) did not use the result of Kondo (1975) to evaluate (24b) but indicated that (24c) agrees well with the data he collected.

In a boundary layer model proposed by Cardone (1969), a relation is assumed

$$z_o = 0.684/u_* + 4.285 \times 10^{-5} u_*^2 - 4.43 \times 10^{-2} \tag{25}$$

Combining this relation with (21), a relation between C_D and U can be obtained.

In evaluating the above relations, the surface drift velocity is neglected by the investigators, i.e., U_s is assumed to be zero. The drag coefficient and roughness parameter obtained with the $U_s = 0$ assumption are related to the actual values, C_D' and z_o',

$$C_D^{-\frac{1}{2}} = C_D'^{-\frac{1}{2}} + U_s/u_* \tag{26}$$

$$z_o = z_o' \exp\ (-kU_s/u_*). \tag{27}$$

The ratio U_s/u_* is a parameter of wind-wave coupling and its effect on the drag has been discussed by Kitaigorodskii (1973) and Davidson (1974). Wu (1975) found by laboratory experiments that this ratio decreases gradually as the fetch increases and approaches approximately the relation $U_s = 0.55\ u_*$.

Figure 6 shows the wind-speed dependence of the drag coefficient for the four models (24a), (24b), (24c), and (26).

Table 4: Parameters in Expressions for Neutral Bulk Transfer Coefficients

U_{10} (m s^{-1})	p	q	r
0.3 to 2.2	0	1.08	-0.15
2.2 to 5	0.771	0.0858	1
5 to 8	0.867	0.0667	1
8 to 25	1.2	0.025	1
25 to 50	0	0.073	1

10. THE STABILITY FUNCTIONS

The surface stress and the surface heat flux can be determined from U and $(T - T_o)$ by integrating the mean profiles.

$$\hat{U}/u_* = [\ln(\hat{z}/z_o) - \psi_U]/k \qquad (28)$$

$$(T - T_o)/T_* = [\ln(\hat{z}/z_o) - \psi_T]/\alpha_N k, \qquad (29)$$

where $T_* = -H_o(c\rho u_*)$, $\alpha_N = K_H/K_M$ at neutral stability, K_H and K_M are the turbulent diffusivities for heat and momentum, c is the isobaric specific heat, U and T are the mean wind speed and potential temperature at height z, and T_o is the temperature at z_o given by the extrapolation of (29). The evaluation of z_o has been discussed in section 9. In this section we investigate the stability functions ψ_U and ψ_T.

For a diabatic surface layer, similarity theory suggests that the non-dimensional gradients are functions of the stability parameter, ζ.

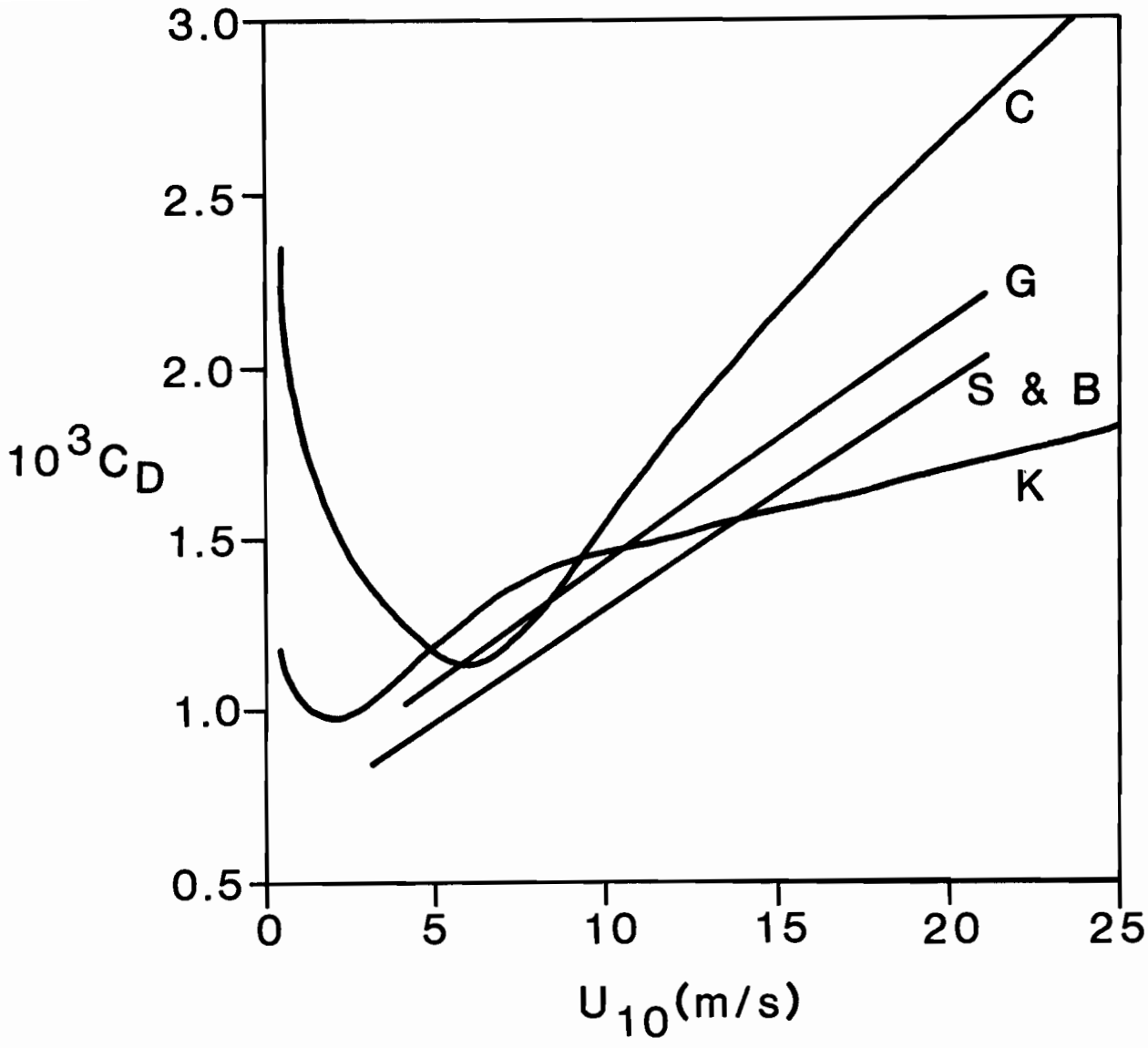

Figure 6 -- A plot of the neutral drag coefficient as a function of wind speed for four different assumptions (K = Kondo, S + B = Smith and Banke, G = Garratt, C = Cardon).

$$kz(\partial U/\partial z)/u_* = \phi_U(\zeta) \tag{30}$$

$$\alpha_N kz(\partial T/\partial z)/T_* = \phi_T(\zeta), \tag{31}$$

where $\zeta = z/L$[1] and L is the Obukhov's length. Combination of (28), (29), (30) and (31) gives

$$\psi_U = \int_{\zeta_o}^{\zeta}[(1 - \phi_U)/\zeta']d\zeta'$$

$$\psi_T = \int_{\zeta_o}^{\zeta}[(1 - \phi_T)/\zeta']d\zeta'.$$

Under unstable conditions, the KEYPS model (Panofsky et al., 1960) proposes

$$\phi_U^4 - a\zeta\phi_U^3 = 1. \tag{32}$$

The adjustable constant a is taken to be 18 following Panofsky et al. (1960).

If the effect of moisture fluctuations on density is neglected, the Obukhov's length is defined as

$$L = -Tu_*^2/(kgT_*). \tag{33}$$

With the assumption that K_H/K_M is constant and equal to unity, $\phi_T = \phi_U = \phi$, $\psi_T = \psi_U = \psi$ and

$$L = -u_*^2 T[\ln(z/z_o) - \psi_o/k^2 g(T - T_o)]. \tag{34}$$

Recently, profile measurements in the surface layer have been successfully described by the Businger-Dyer model:

$$\psi_U = (1 - a_U\zeta)^{-1/4} \tag{35}$$

$$\phi_T = (1 - a_T\zeta)^{-1/2}. \tag{36}$$

[1]Note a new definition for ζ.

Results from the Kansas experiment (Businger et al., 1971) give $a_U = 15$, $a_T = 9$ while $k = 0.35$ and $\alpha_N = 1$. However, Paulson (1970), with the assumption that $k = 0.4$ and $\alpha_N = 1$, obtained $a_U = a_T = 16$ in his analysis of Kerang data, in close agreement with Dyer (1967). The Businger-Dyer model differs from the KEYPS model in that the B-D model allows for the variation of K_H/K_M with stability. Paulson (1970) found that both models describe velocity distribution equally well but the B-D model gives better representation in temperature distribution. The two models also give different dependence of U and T on z when free convection is approached (see Businger et al., 1971 and Businger, 1973 for further discussion). Both the Kansas and Kerang data are measured over land. The B-D model has also been found to represent measurements over ocean in the Spanish Bank experiment (Miyake et al., 1970), the Indian Ocean experiment (Badgley et al., 1972), and the BOMEX experiment (Paulson et al., 1972).

Figure 7 shows the stress as a function of wind speed for unstable stratification of 3°C for the three models. $z_o(u_*)$ relations from Cardone (1969) have been used in these calculations. Figure 8 shows the rate of heat flux evaluated for a range of air-sea temperature differences. T_{10} and U_{10} are potential temperature and wind speed at 10 m. Stresses evaluated with the B-D model with $k = 0.4$ are about 1 percent lower than those evaluated with the KEYPS model at moderate wind speed but increase to 8 percent at 1 m s^{-1} wind. With $k = 0.35$ the stress is about 30 percent lower. The heat fluxes evaluated by the B-D model with the two sets of constants are about 6 and 13 percent lower than those with the KEYPS model.

Under stable conditions, the log-linear model which was obtained by dropping the higher order terms in the power expansion of ϕ_U and ϕ_T are used:

$$\phi_U = 1 + b_U\zeta \qquad (37)$$

$$\phi_T = 1 + b_T\zeta.$$

Cardone (1969) uses the values $k = 0.4$, $\alpha_N = 1$, $b_T = b_U = 7$. Similar values have been used by McVeil (1963) and others. Businger et al. (1971) suggested $k = 0.35$, $\alpha_N = 1.35$, $b_U = 4.7$ and $b_T = 6.35$. However, the log-

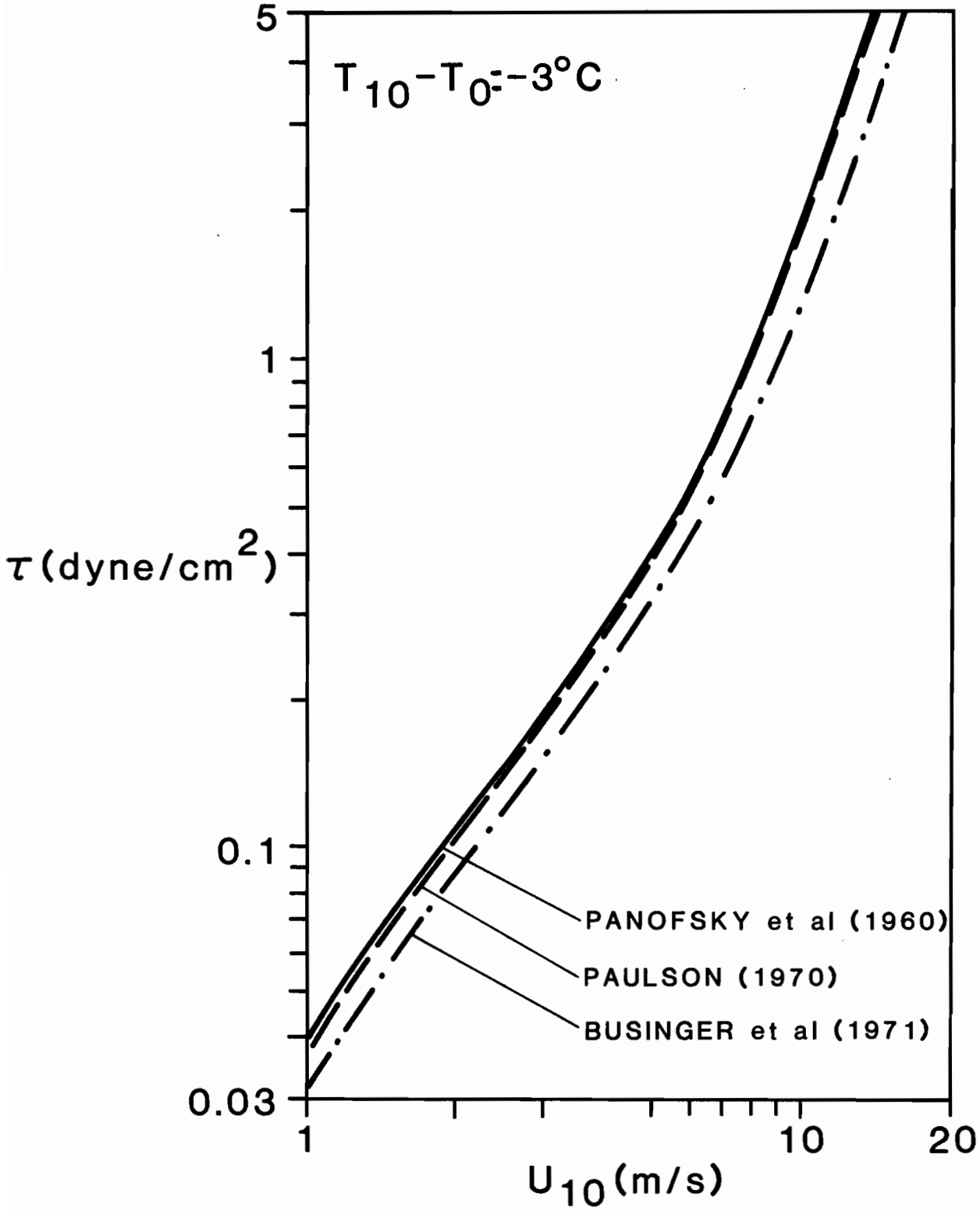

Figure 7 -- Stress versus wind speed for unstable stratification for three stability function models.

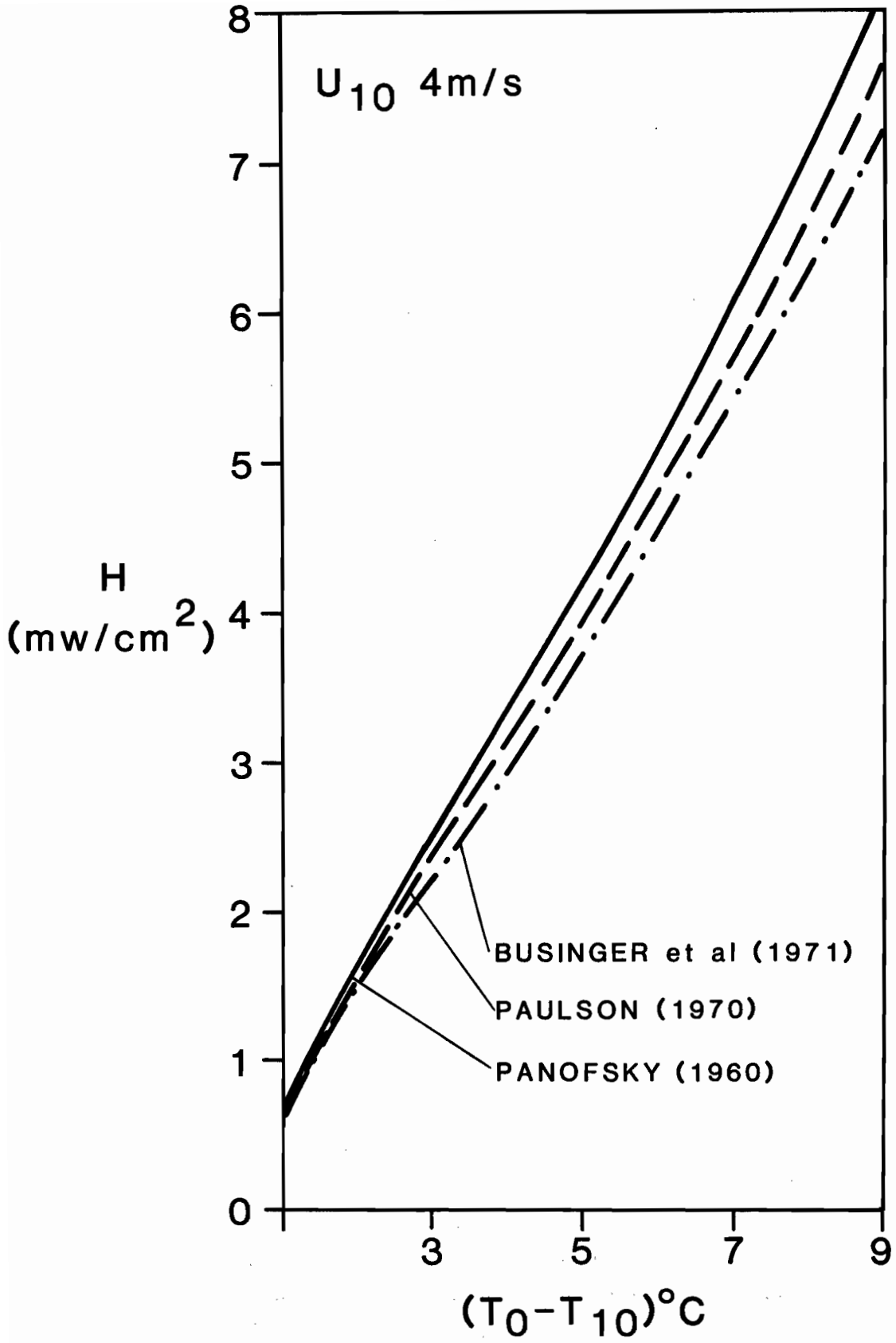

Figure 8 -- Heat flux as a function of unstable air sea temperature for three stability models.

linear model has its limitations. From the definition,

$$\zeta = \alpha_N \phi_U^2 Ri/\phi_T, \tag{38}$$

where $Ri = g(\partial T/\partial z)^2$ is the Richardson number. For $b_U = b_T = b$

$$\zeta = \frac{A}{1 + B},$$

where $A = \alpha_N Ri$, $B = \alpha_N Ri\ b$ and ζ can be solved by fix-point iterations only if

$$B < 1$$

and

$$Ri < (\alpha_N b)^{-1}. \tag{39}$$

The quantity $(\alpha_N b)^{-1}$ is also the asymptotic value of Ri as ζ increases in value.

The criterion (39) is equivalent to

$$gz(T - T_0)/(TU^2) < (\alpha_N b)^{-1}.$$

For z = 10 m, g = 981 cm s^{-1}, $\alpha_N = 1$, b = 7, T = 280°K, in order to have a realistic solution, $(T - T_0)/U^2 < 4.1 \times 10^{-5}$. In other words, there is no solution when $U_{10} < 157$ cm s^{-1} for $(T_{10} - T_0) = 1$°C and when $U_{10} < 221$ cm s^{-1} for $(T_{10} - T_0) = 2$°C. Kondo (1975) suggested

$$\phi = 1 + 6\zeta/(1 + \zeta), \tag{40}$$

which is not subjected to the above condition for a solution.

The stresses evaluated with these models are compared in Figure 9. The stress evaluated with Cardone (1969) is lower than that evaluated with Kondo's model by 3 percent at a wind speed of 10 m s^{-1} and by 59 percent at a wind speed of 2 m s^{-1}. With the representation suggested by Businger et al. (1971), which means a different value of von Karman's constant, the stress is about 40 percent lower than the Kondo representation. Most of this is due to the smaller k.

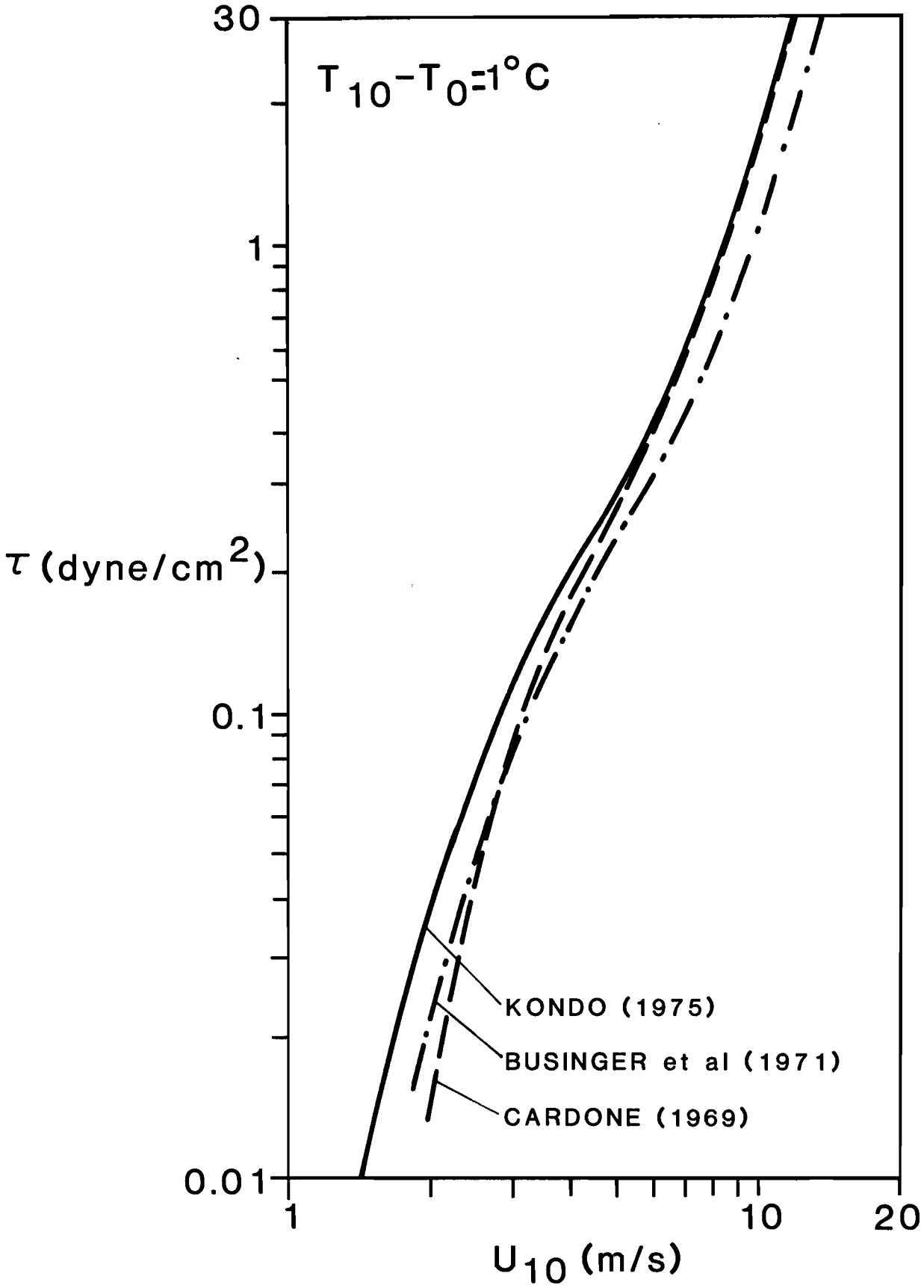

Figure 9 -- Stress versus wind speed for stable stratification for three stability function models.

Over water, the effect of moisture fluctuations on buoyancy may be important. The Obukhov length can be redefined to include this effect:

$$L = T_v u_*^2/(gkT_{v*}),$$

where $T_v = T(1 + 0.61Q)$ and $T_{v*} = T_*(1 - 0.61Q) + 0.61TQ_*$, $Q_* = -E/u_*$, E is the moisture flux, Q is the specific humidity at z. The moisture flux can be determined from the humidity profile

$$(Q - Q_O)/Q_* = [\ln(z/z_o) - \psi_Q]\ (\alpha_N' k)^{-1},$$

where $\alpha_N' = K_E/K_M$ at neutral stability and K_E is the turbulent diffusivity of moisture. Assuming $\alpha_N' = \alpha_N$, $\psi_Q = \psi_T$, the stress and heat flux can be evaluated for different values of relative humidity. The percentage difference between the values evaluated with the effects of moisture included and those with the effects excluded are shown in Tables 5 and 6. The difference in stress decreases with increasing wind speed because at low wind speed the buoyancy production becomes increasingly important relative to the shear production. The difference is larger the drier the air.

The sea-surface temperature T_s, rather than T_o, is generally available. Figure 10 shows that under slightly unstable conditions, the heat flux extimated by assuming $T_o = T_s(z_T = z_o)$ differs from those extimated by including a sublayer model (Liu, 1978) by 3 percent in low wind speed up to 27 percent for 20 m s^{-1} winds.

Table 5: **Percentage Difference Between the Stress Evaluated with the Effects of Moisture on Buoyancy Included and those with the Effects Excluded.**

$T_0 = 10°C$

	$T_{10} - T_0 = 1°C$			$T_{10} - T_0 = -3°C$		
	R.H.			R.H.		
U_{10} (m s^{-1})	100%	60%	0%	100%	60%	0%
1	20	64	159	1	4	6
5	1	6	18	1	2	3
10	0.3	2	7	1	1	4

$T_0 = 25°C$

	$T_{10} - T_0 = 1°C$			$T_{10} - T_0 = -3°C$		
	R.H.			R.H.		
U_{10} (m s^{-1})	100%	60%	0%	100%	60%	0%
1	13	5	169	3	8	14
5	-0.3	17	4	2	4	8
10	-8	7	10	1	5	12

Table 6: **Percentage Difference Between the Heat Flux Evaluated with the Effects of Moisture on Buoyancy Included and those with the Effects Excluded** (U_{10} = 5 m s^{-1})

	T_0 = 10°C			T_0 = 25°C		
	R.H.			R.H.		
$T_{10} - T_0$	100%	60%	0%	100%	60%	0%
-3°C	1	2	3	2	4	7
1°C	1	7	8	-0.3	18	28

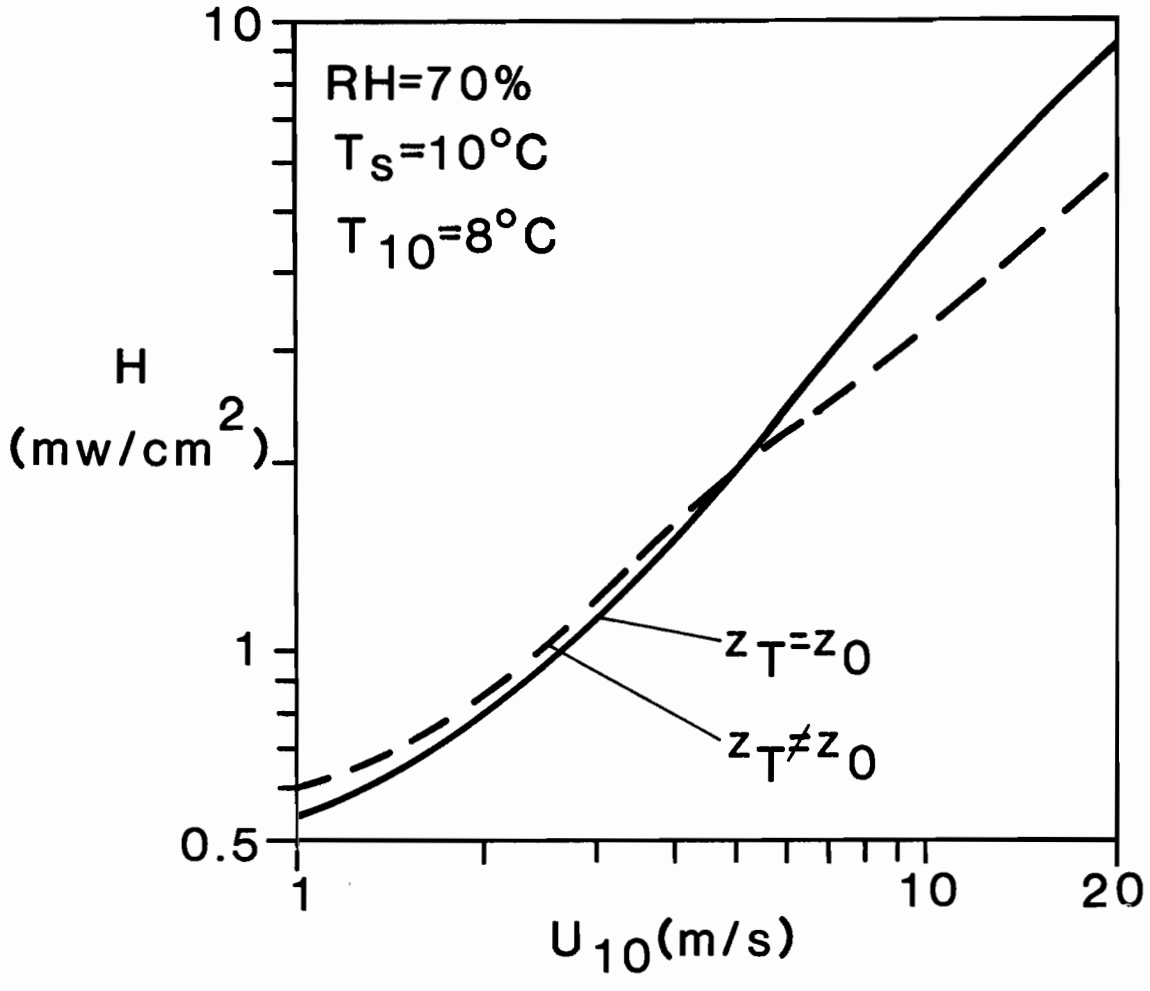

Figure 10-- Heat flux as a function of wind speed with the assumption of a sublayer adjacent to the surface, $z_T \neq z_o$.

REFERENCES (APPENDIX A)

Badgley, F. I., C. A. Paulson and M. Miyake (1972): Profile of wind temperature and humidity over the Arabian Sea, International Indian Ocean Expedition. Meteor. Monograph, 6, 66.

Brown, R. A. (1970): A secondary flow model for the planetary boundary layer. J. Atmos. Sci., 27, 742-757.

Brown, R. A. (1972): The inflection point instability problem for stratified rotating boundary layers. J. Atmos. Sci., 29, 850-859.

Brown, R. A. (1974): Analytical Methods in Planetary-Layer Modelling, Adam Hilger Ltd., London, and Halsted press, John Wiley & sons, N. Y. 148 pp.

Brown, R. A. (1978): Similarity parameters from first-order closure and data. Boundary-Layer Meteorol., 14, 381-396.

Businger, J. A. (1973): A note of free convection. Boundary-layer Meteorol., 4, 323-326.

Businger, J. A., J. C. Wyngaard, Y. Izumi and E. F. Bradley (1971): Flux profile relationships in the atmospheric surface layer. J. Atmos. Sci., 28, 181-189.

Cardone, V. J. (1969): Specification of the wind distribution in the marine boundary layer for wave forecasting. Report GSL-TR69-1, New York Univ., School of Engineering and Science, 131 pp.

Charnock, H. (1955): Wind stress on a water surface. Quart. J. Royal Meteor. Soc., 81, 639-640.

Davidson, K. L. (1974): Observational results on the influence of stability and wind-wave coupling on momentum transfer and turbulent fluctuations over ocean waves. Boundary-Layer Meteorol., 6, 305-331.

Dyer, A. J. (1967): The turbulent transport of heat and water vapour in an unstable atmosphere. Quart. J. Roy. Meteor. Soc., 93, 501-508.

Garrett, J. R. (1977). Review of drag coefficients over oceans and continents. Mon. Weather Rev., 105, 915-929.

Hasse, L. (1970): On the determination of vertical transports of momentum and heat in the atmospheric boundary layer at sea. Technical Report 188, School of Oceanography, Oregon State University.

Kitaigorodskiy, S. A. (1973). The Physics of Air-sea Interaction, Israel Program for Scientific Translation, Jerusalem.

Kondo, J. (1975): Air-sea bulk transfer coefficients in diabatic condition, Boundary-Layer Meteorol., 9, 91-112.

Kondo, J., Y. Fujinawa and G. Naito (1973): High frequency component of ocean waves and their relation to aerodynamic roughness. J. Phys. Oceanogr., 3, 197-222.

Liu, W. T. (1978): The molecular effects of air-sea exchanges. Ph.D. dissertation, University of Washington, Seattle.

Liu, W. T. and J. Businger (1975): Temperature profile in the molecular sublayer near the interface of a fluid in turbulent motion. Geophys. Res. Let., 2, 403-404.

Liu, W. T., K. B. Katsaros and J. A. Businger (1979): Bulk parameterization of air-sea exchanges of heat and water vapor including the molecular constraints at the interface, submitted to J. Atmos. Sci. for publication.

McVeil, G. E. (1964): Wind and temperature profiles near the ground in stable stratification. Quart. J. Roy. Meteor. Soc., 90, 136-146.

Miyake, M., M. Donelan, G. McBean, C. Paulson, F. Badgley and E. Leavitt (1970): Comparison of turbulent fluxes determined by profile and eddy correlation techniques. Quart. J. Roy. Meteor. Soc., 96, 132-137.

Nikvradse, J. (1933): Laws of flow in rough pipes, N.A.C.A. Technical Memorandum 1292.

Paulson, C. A. (1970): The mathematical representation of wind speed and temperature profiles in the unstable atmospheric surface layer. J. Appl. Meteorol., 9, 857-861.

Paulson, C. A., E. Leavitt and R. G. Fleagle (1972): Air-sea transfer of momentum, heat, and water determined from profile measurements during BOMEX. J. Phys. Oceanogr., 2, 487-497.

Panofsky, H. A., A. K. Blackadar and G. E. McVeil (1960): The diabatic wind profile. Quart. J. Roy. Meteor. Soc., 86, 390-398.

Smith, S. D. (1973): Thrust-anemometer measurements over the sea reexamined, Report 73-1, Bedford Inst. Oceanography.

Smith, S. D. (1974): Eddy flux measurements over Lake Ontario. Boundary-Layer Meteor., 6, 235-256.

Smith, S. D. and E. G. Banke (1975): Variation of the sea surface drag coefficient with wind speed. Quart. J. Roy. Meteor. Soc., 101, 665-673.

Wu, J. (1969): Wind stress and surface roughness at the air-interface. J. Geophys. Res., 74, 444-455.

Wu, J. (1975): Wind-induced drift currents. J. Fluid Mech., 68, 49-70.

Wu, J. (1979): Wind-wave interaction. Phys. Fluid, 13, 1926-1930.

Appendix B: DERIVATION OF CARDONE MODEL

Cardone's model, an extension of Blackadar (1965), separates the boundary layer into two regions: a surface layer and an Ekman layer. The surface layer is assumed to be a constant-flux layer in which the eddy viscosity variation with height is specified as a function of the atmospheric stability according to the Monin-Obukhov similarity theory. The upper Ekman layer is assumed to have a constant eddy viscosity, K_m (Fig. B1) (Cardone 1969).

The surface layer assumes the standard Monin-Obukhov similarity hypothesis that the non-dimensional wind speed and potential temperature gradients defined by

$$\phi_u = \frac{kz}{u_*} \frac{\partial u}{\partial z}$$
$$\phi_\theta = \frac{z}{\theta_*} \frac{\partial \theta}{\partial z} \qquad \text{(B1)}$$

are universal functions of the stability parameter L or L', where

L $-u_*^3 C_p \rho T/(kgH)$, the Monin length

u mean wind speed

z vertical space coordinate

T mean temperature

k von Karman's constant (=0.4)

u_* $(\tau/\rho)^{\frac{1}{2}}$, friction velocity

H $C_p \rho \overline{w'T'}$, turbulent heat flux

θ_* $-H/(ku_*\rho C_p)$, a scaling temperature

θ $T + \Gamma z$, potential temperature

Γ g/C_p, adiabatic lapse rate

g acceleration of gravity

C_p specific heat at constant pressure

ρ air density

τ tangential stress

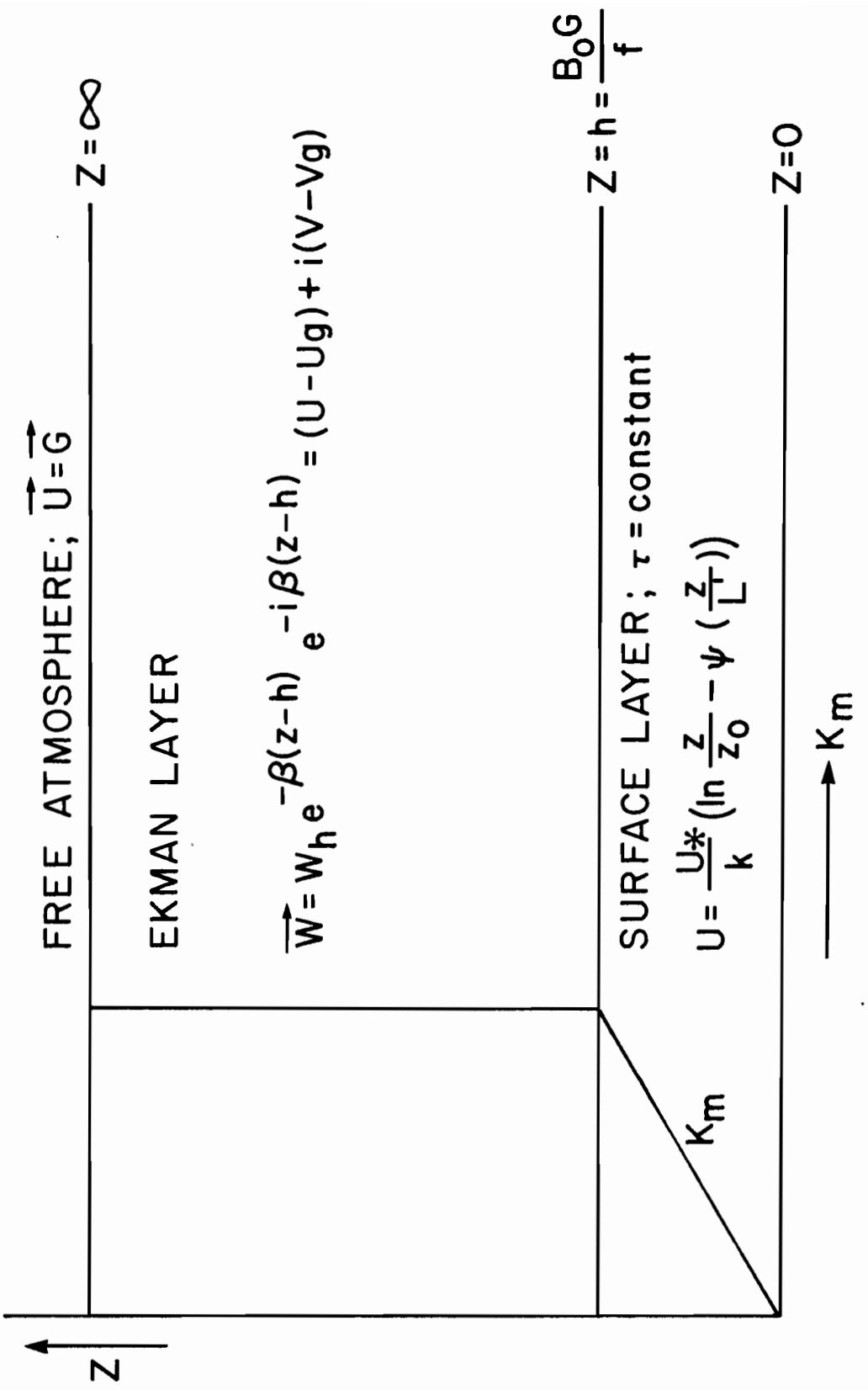

Figure B1. Model of the atmospheric surface boundary layer.

K_m $u_*^2/(\partial u/\partial z)$, turbulent transfer coefficient for momentum

K_H $-H/(\rho C_p\ \partial\theta/\partial z)$, turbulent transfer coefficient for heat

a_h K_H/K_m, reciprocal of the turbulent Prandtl number

L' $a_h L$.

Integrating the non-dimensional gradients gives:

$$u = \frac{u_*}{k}\ [\ell n\ (z/z_o) - \psi_u\ (z/L')] \tag{B2}$$

$$\theta = \theta_s + \frac{\theta_*}{a_h}\ [\ell n\ (z/z_o) - \psi_\theta(z/L')],$$

where z_o is the roughness length and

$$\psi_u\ (z/L') = \int_o^\xi \frac{1 - \phi_u(\xi)}{\xi}\ d\xi,\ \xi = \frac{z}{L'}\ . \tag{B3}$$

Under the assumption that the profile of wind and temperature are similar up to the anemometer height "a", i.e., $a_h \simeq 1$, $\phi_\theta \simeq \phi_u$, the stability length can be defined in terms of an anemometer height temperature

$$L' = a_h L = \frac{U_* T \partial u/\partial z}{kg\ \partial\theta/\partial z} \simeq \frac{U_*^2 \overline{\theta}\ [\ell n\ (a/z_o) - \psi_u\ (a/L')]}{k^2 g\ (\theta_a - \theta_s)}\ . \tag{B4}$$

For a/L' small, with "a" a small fraction of the surface layer height, this is a good approximation. However, it would be an easy matter to carry both ψ_u and ψ_θ. Our listing contrasts with Cardone's in that we have replaced a = 19.5 m with a = 10.0 m. Cardone uses the KEYPS representation for ϕ which interpolates between neutral stability and free convection:

$$\phi_u^{\,4} - \alpha'(z/L')\ \phi_u^{\,3} - 1 = 0, \tag{B5}$$

with $\alpha' = 18$.

This is solved by defining an intermediate variable, the Richardson number:

$$R_i = \frac{g}{\theta}\ \frac{\frac{d\theta}{dz}}{\left(\frac{du}{dz}\right)^2} = \frac{z}{L'}\ \frac{1}{\phi_u(z/L')}\ ,$$

so that

$$\frac{z}{L'} = \frac{R_i}{(1-\alpha' R_i)^{\frac{1}{4}}}$$

and

$$\phi_u = \frac{1}{(1 - \alpha' R_i)^{\frac{1}{4}}} .$$

The KEYPS representation implies that both u and θ vary asymptotically as $z^{-1/3}$. The B5 relation implies

$$\psi(z/L') = 1-\phi-3\ell n\phi + 2\ell n(\frac{1 + \phi}{2}) + 2\tan^{-1}\phi - \frac{\Pi}{2} + \ell n(\frac{1 + \phi^2}{2}). \qquad (B6)$$

An alternate form is the Businger-Dyer (B-D) profiles:

$$\phi_u = [1 - \alpha'(z/L)]^{-\frac{1}{4}}$$

$$\phi_\theta = [1 - \alpha'(z/L)]^{-\frac{1}{2}}$$

$$\psi_u = 2\ell n [(1 + x)/2] + \ell n [(1 + x^2)/2] - 2 \tan^{-1} x + \frac{\Pi}{2}$$

$$\psi_\theta = 2\ell n [(1 + x^2)/2], \qquad (B7)$$

where $x = (1 - \alpha' z/L)^{\frac{1}{4}}$.

The ψ_θ profile is important only to level "a" (i.e., in defining L'); however, the choice of the ψ_u profile is critical in matching velocities at the top of the surface layer. For stable boundary layers, Cardone has

$$\phi_u (z/L') = 1 + \beta' z/L'$$

$$\psi_u (z/L') = -\beta' z/L' \qquad (B8')$$

with $\beta' = 7$.

The linear profile in B8' is generally limited to $z/L' < 0.3$ which in practice can be $\theta_a - \theta_s < 2°C$. To extend the stable range we replace B8' by

$$\phi_u (z/L') = 1 + \frac{\beta'(z/L')}{1 + z/L'}$$

$$\psi (z/L') = -\beta' \ell n(1 + z/L'). \qquad (B8)$$

Wave development is considered indirectly through the dependence of surface roughness upon u_* in the following relation:

$$z_o = 0.684/u_* + 4.285 \times 10^{-5} u_*^2 - 4.43 \times 10^{-2}, \qquad (B9)$$

where z_o is in cm and u_* in cm s^{-1}. The relation B9 implies a viscous sublayer for small u_* and the Charnock (1955) relation ($z_o = a_c u_*^2/g$) for large u_*.

Equation B9 along with B2 implies a variation of the drag coefficient at neutral stability, $[C_{10} = k^2/\ell n(10m/z_o)]$, as shown in Figure B2.

The structure of the planetary boundary layer is shown in Figure B1. A key assumption is specification of the height of the surface layer as

$$h = \frac{B_o G}{f} \tag{B10}$$

where G is the wind speed at the top of the boundary layer, f is the Coriolis parameter, and B_o is an assignable constant, 3.0×10^{-4} (Blackadar, 1965). Note that h is independent of stability. The outer layer is governed by an Ekman equation with constant eddy viscosity

$$if\vec{v} = if\vec{G} + K_m \frac{\partial^2 \vec{v}}{\partial z^2} , \tag{B11}$$

with boundary conditions

$$\vec{v} \to G \text{ at } z \to \infty$$

$$\vec{v} \frac{\partial \vec{v}}{\partial z} , \vec{\tau} \text{ continuous at } z = h. \tag{B12}$$

The solution to B11 in terms of a velocity deficit is

$$W = (u - u_g) + i(v - v_g)$$

$$W = W_h \exp[-\beta(1 + i)(z - h)], \tag{B13}$$

with W_h being the deficit between the wind speed at the top of the surface layer and the geostrophic velocity and with $\beta = f/(2K_m)$.

Figure B3 shows the barotropic boundary condition at the internal boundary height. Differentiating B12 with respect to z gives

$$\frac{\partial W}{\partial z} = -(1 + i)\beta W. \tag{B14}$$

Since $\partial\vec{u}/\partial z$ is parallel to $\vec{u}$ and $\partial\vec{u}/\partial z|_h = \partial\vec{W}/\partial z|_h$, the angular relationship between $\vec{u}_h$ and $\vec{w}_h$ is established as

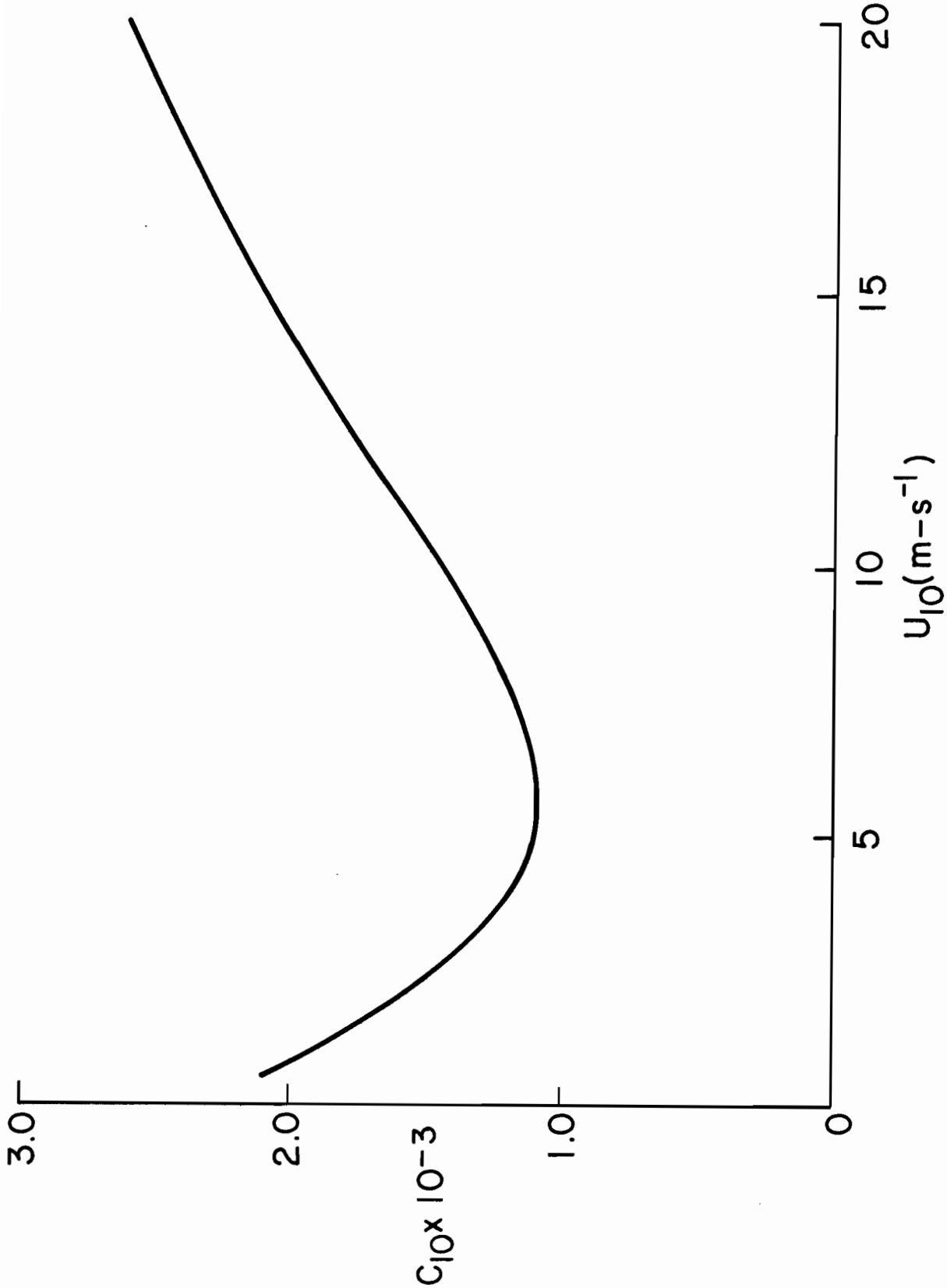

Figure B2. Drag coefficient with respect to 10 m as a function of 10-m wind speed for neutral conditions and roughness parameter specification Eq. B9.

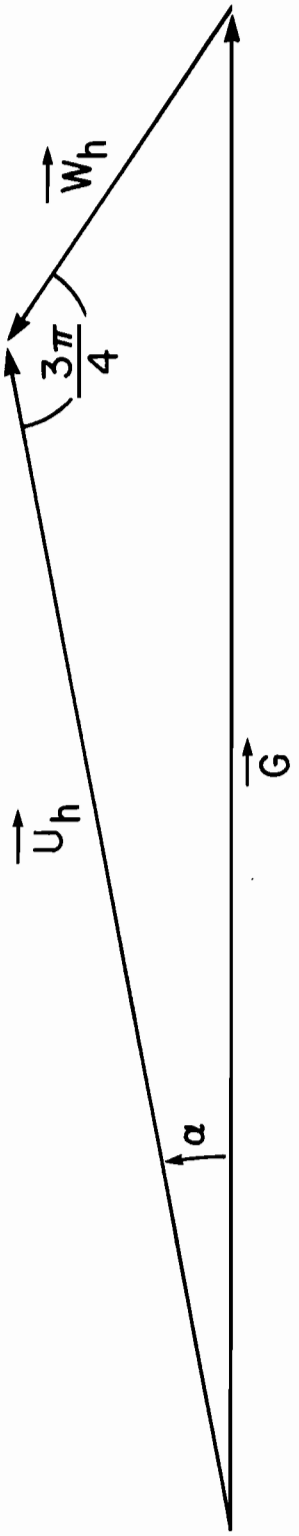

Figure B3. Barotropic boundary condition on the internal boundary surface.

$$\frac{\vec{u}_h}{u_h} = -(1 + i)\frac{\vec{W}_h}{W_h} . \tag{B15}$$

By using the law of sines on Figure B3

$$\frac{u_h}{G} = \sqrt{2}\sin(\frac{\Pi}{4} - \alpha), \tag{B16}$$

and again

$$\frac{W_h}{G} = \sqrt{2}\sin\alpha. \tag{B17}$$

The profile B1 in the surface layer implies

$$K_m = \frac{k\, u_* \, z}{\phi_u(z/L')} \quad z \leq h. \tag{B18}$$

This relation combined with B10 and B12 implies

$$K_m = \frac{k\, u_* \, B_o G}{f\phi_u(z/L')} \quad z \geq h \tag{B19}$$

and

$$\beta = f\sqrt{\frac{\phi_u(z/L')}{2k\, u_* \, B_o G}} . \tag{B20}$$

The mixing coefficient in the upper layer is a function of stability in the sense that its magnitude is determined by the value where the profile B18 intersects height h and is larger for unstable stability and smaller for a stable regime. At z = h

$$u_h = \frac{u_*}{k}[\ell n \frac{B_o G}{f z_o} - \psi_u(h/L')] \tag{B21}$$

$$\left.\frac{\partial u}{\partial z}\right|_{-h} = \frac{u_* f \phi_u(h/L')}{k\, B_o G} \tag{B22}$$

$$\left|\left.\frac{\partial u}{\partial z}\right|_{+h}\right| = \left|\left.\frac{\partial w}{\partial z}\right|_{+h}\right| = \sqrt{2}\,\beta|W_h| . \tag{B23}$$

B22 and B23 imply

$$|W_h| = u_* f\, \phi_u(h/L')/(\sqrt{2}\, k\, B_o G\, \beta). \tag{B24}$$

Combining B17 and B24 gives

$$\frac{u_*}{G} = [2k\ B_o\ \sin^2\alpha/\phi_u(h/L')]^{1/3}, \tag{B25}$$

and combining B16 and B21 gives

$$\frac{u_*}{G} = \sqrt{2}\ k\ \sin(\frac{\Pi}{4} - \alpha)/[\ell n\ \frac{B_o G}{f z_o} - \psi(h/L')]. \tag{B26}$$

B25 and B26 along with the definition of z_o and L' (B4 and B9) are solved by iteration.

The baroclinic derivation deviates from the barotropic in that the shear in the surface layer is matched to the sum of the geostrophic shear and the shear of the deficit velocity. Several secondary variables are defined, but the relations are straightforward in terms of the triangle geometry of the vector balance at height h. It is convenient to define a parameter

$$p = \frac{u_h}{\left|\frac{\partial u}{\partial z}\right|_h} = \frac{B_o G}{f\phi_u}\ [\ell n\ \frac{B_o G}{f z_o} - \psi]. \tag{B27}$$

From this definition and boundary condition B12,

$$u_h = p[\frac{\partial G}{\partial z} + \frac{\partial W}{\partial z}]_h. \tag{B28}$$

In the same way as Figure B3 we can define Figure B4 to apply at level h with η as the angle between the thermal and geostrophic wind. By differentiation of W we again obtain a relation similar to B23:

$$p\left|\frac{\partial W}{\partial z}\right|_h = \sqrt{2}'\ p'\ \left|W_h\right| \tag{B29}$$

with

$$p' = \left(\frac{f^2\ \phi_u}{2k\ u_*\ B_o G}\right)^{\frac{1}{2}}\ p.$$

The magnitude of the thermal wind is defined by

$$r = \frac{1}{f}\ \left|\frac{\partial G}{\partial z}\right|\ . \tag{B30}$$

One can construct a relation similar to B29 by setting

$$p\left|\frac{\partial G}{\partial z}\right| = r'G \tag{B31}$$

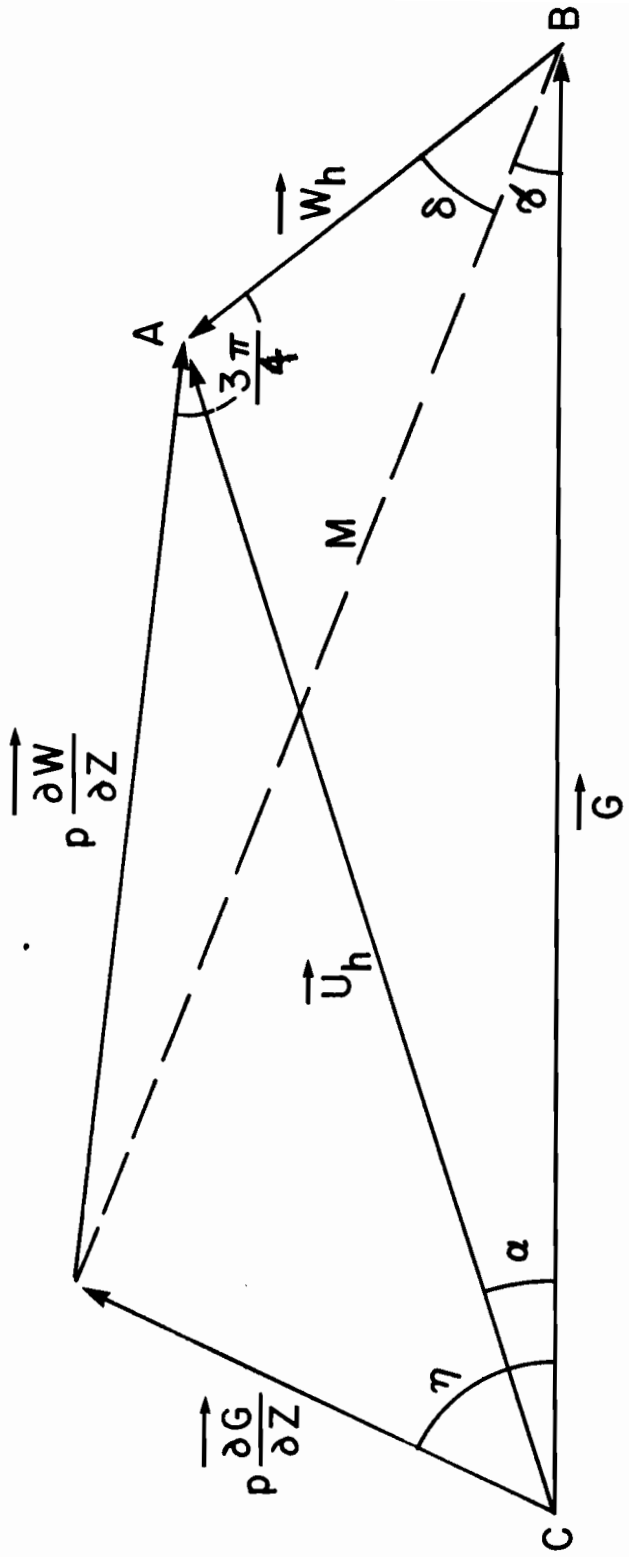

Figure B4. Baroclinic boundary condition on the internal boundary surface.

with

$$r' = \frac{r\,B_o}{\phi_u}\left[\ell n\,\frac{B_o G}{f z_o} - \psi_u\right].$$

From the law of cosines of triangle ABD with interior angle $3\pi/4$,

$$M^2 = p\left|\frac{\partial W}{\partial z}\right|^2 + W_h^{\,2} - 2p\,\frac{\partial W}{\partial z}\,W_h\cos\frac{3\pi}{4} \tag{B32}$$

or

$$M^2 = W_h^{\,2}\,s^2$$

where

$$s^2 = 2p'^2 + 2p' + 1.$$

From the law of cosines of triangle BCD with interior angle η,

$$M^2 = (P\,\frac{\partial G}{\partial z})^2 + G^2 - 2P\left|\frac{\partial G}{\partial z}\right|\,G\cos\eta$$

or

$$M^2 = W_h^{\,2}s^2 = G^2q^2 \tag{B33}$$

where

$$q^2 = 1 + r'^2 - 2r'\cos\eta.$$

From the law of sines for ABD and B32,

$$\sin\delta = \frac{p(\partial W/\partial z)}{\sqrt{2}\,M} = \frac{P'}{s}\,, \tag{B34}$$

and from the law of sines for BCD and B33,

$$\sin\gamma = \frac{p\partial G/\partial z}{M}\sin\eta = \frac{R'}{q}\sin\eta. \tag{B35}$$

The law of sines on ABC gives

$$u_h = W_h\,\frac{\sin(\delta + \gamma)}{\sin\alpha}. \tag{B36}$$

The law of cosines on the same triangle taking $(\delta + \gamma)$ as the interior angle gives

$$u_h^2 = G^2 W_h^2 - 2GW_h \cos(\delta + \gamma). \tag{B37}$$

Taking α as the interior angle,

$$W_h^2 = u_h^2 + G^2 - 2u_h G \cos\alpha. \tag{B38}$$

Combining B36 and B38 gives

$$\tan\alpha = \frac{2 G W_h \sin(\delta + \gamma)}{G^2 + u_h^2 - W_h^2} \tag{B39}$$

Substituting u_h from B37 and using B33,

$$\tan\alpha = \frac{\sin(\delta + \gamma)}{s/q - \cos(\delta + \gamma)} \tag{B40}$$

Matching B36 to the surface layer velocity at h, i.e., B21, using $W_h = q\ G/s$ from B33, gives

$$\frac{u_*}{G} = \frac{q \sin(\delta + \gamma) k}{s \sin\alpha[\ell n \frac{B_o G}{f z_o} - \psi(\frac{z}{L'})]} . \tag{B41}$$

Secondary variables δ, γ, s, q, p', and p are defined in terms of known parameters. The inflow angle α from B40 and geostrophic drag coefficient from B41 are again solved by iteration along with the equations for z_o and L'. A key point is that the influence of the thermal wind is included by matching the shear rather than an integrated effect through an assumed PBL depth.

Figures B5 through B7 present the plotted dependence of Cardone's model upon air-sea temperature difference, geostrophic wind and thermal wind. The strength of the thermal gradient is $3°/100$ km . Although not shown here, the overall dependencies are quite similar to observations and similarity theory relations.

Modern theory updates Cardone's model by Kondo's surface roughness relations (Appendix A, Garrett 1977) and by Businger-Dyer's stability relations (also Appendix A). Both these relations do not change Cardone's basic PBL theory (Halberstam, 1978), only quantitatively change the results. Both of these relations will be added to Model=8 in the near future.

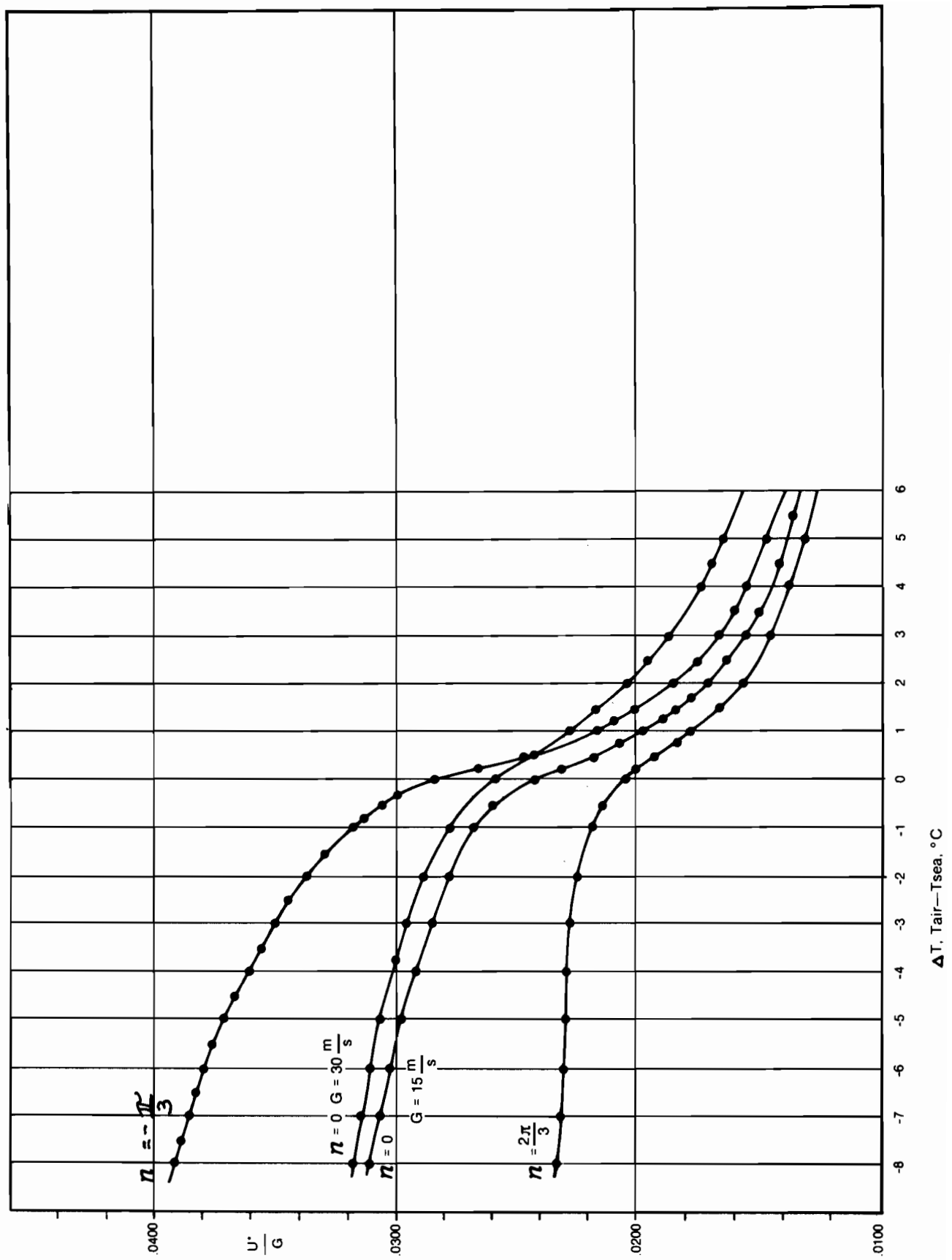

Figure B5. Dependence of the geostrophic drag coefficient on the air-sea temperature difference from Cardone's model. Two curves are given for 15 m s^{-1} and 30 m s^{-1} geostrophic wind and barotropic conditions. The high and low curves are for two orientations of the thermal wind for a surface air temperature gradient of 3°C/100 km.

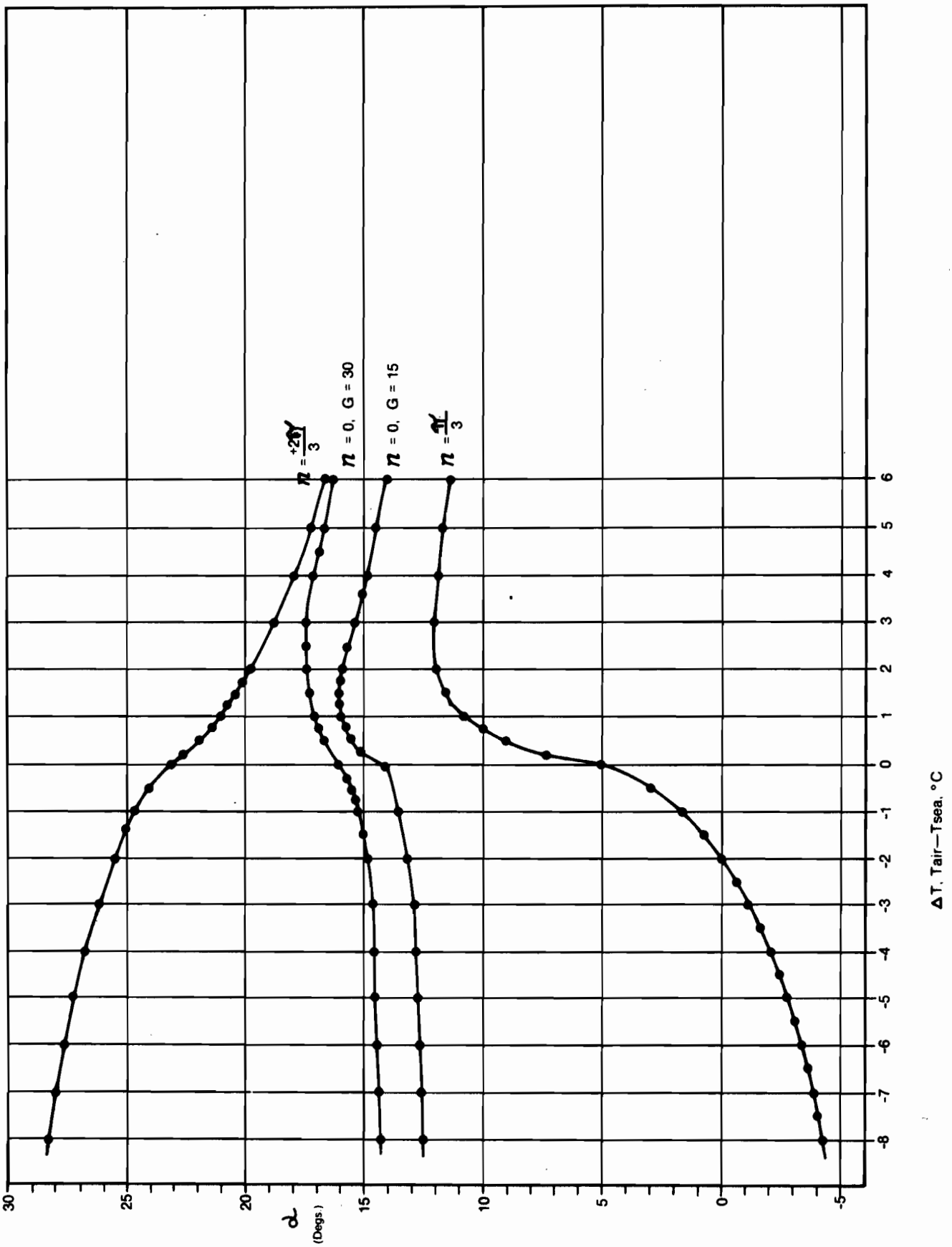

Figure B6. A similar set of curves as in A5 for inflow angle.

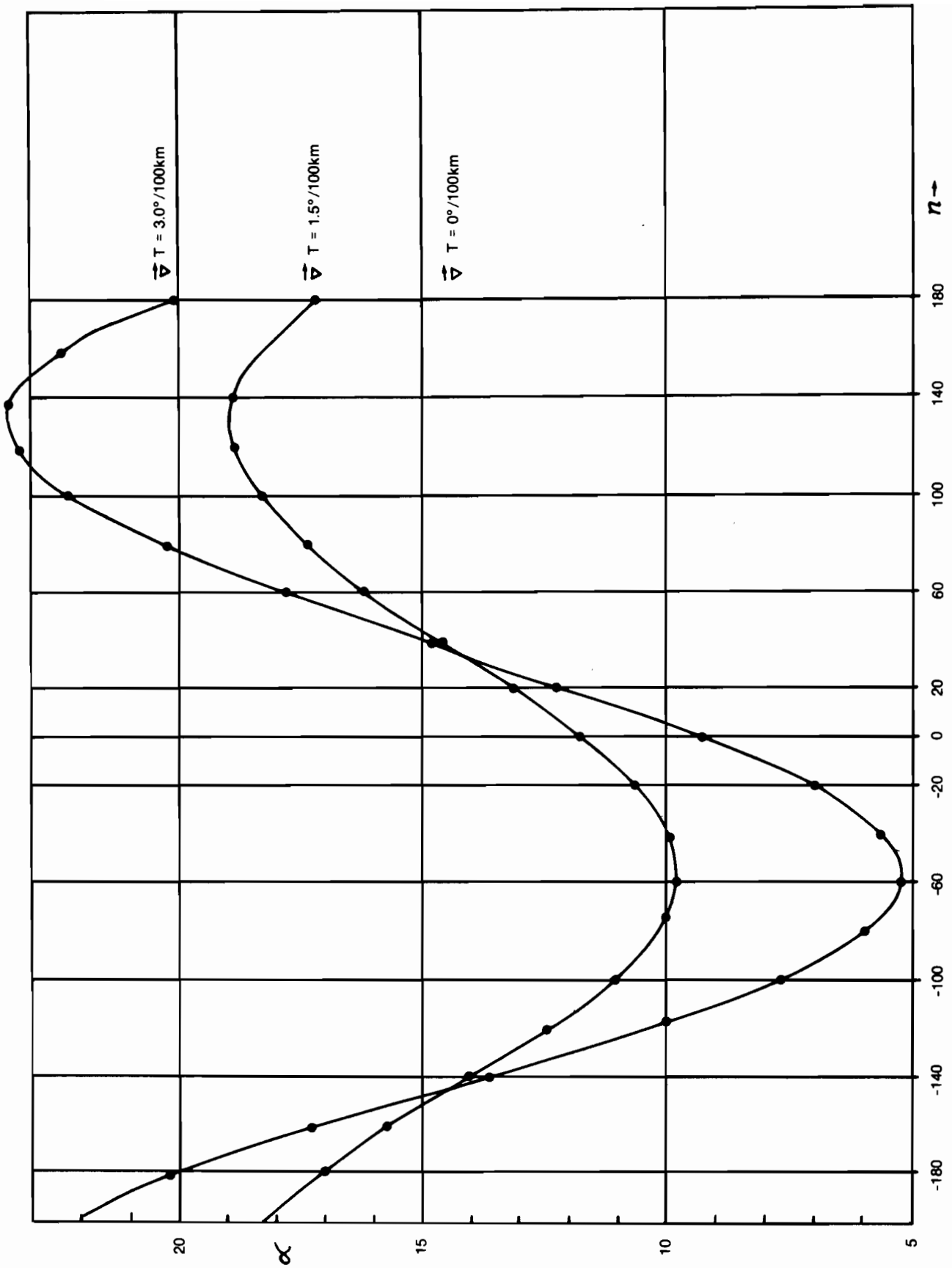

Figure B7. Influence of orientation of the thermal wind on inflow angle for three magnitudes of the thermal wind, 0, 1.5° and 3°C/100 km from Cardone's model. The geostrophic wind magnitude is 15 m s^{-1}.

REFERENCES (APPENDIX B)

Blackadar, A.K.(1965): A simplified two-layer model of the baroclinic neutral atmospheric boundary layer. Air Force Cambridge Res. Lab. Report 65-531, pp 49-65.

Cardone, V.J.(1969): Specification of the wind distribution in the marine boundary layer for wave forecasting. Report GSL-TR69-1, New York University, School of Engineering and Science, 131 pp.

Charnock, H.(1955): Wind stress on a water surface. Quart. J. R. Met. Soc., 81, 639-640.

Garrett, J.R. (1977): Review of drag coefficients over oceans and continents. Mon. Wea. Rev.,, 105, 915-929.

Halberstam, I. (1978): The marine surface layer and its relationship to Seasat-A Scatterometer measurements. Jet Propulsion Laboratory (unpublished manuscript).